SKI Report 02:29

Research

Evaluation of the FRAPCON-3 Computer Code

Lars Olof Jernkvist
Ali Massih

March 2002

ISSN 1104–1374
ISRN SKI-R-02/29-SE

SKI PERSPECTIVE

How this project has contributed to SKI:s research goals

The overall goals for SKI rearch are:

- to give a basis for SKI:s supervision
- to maintain and develop the competence and research capacity within areas which are important to reactor safety
- to contribute directly to the Swedish safety work.

This project has mainly contributed to the strategic goal of giving a basis for SKI:s supervision by means of an independent evaluation of the computer code FRAPCON-3 with respect to its applicability for licensing purposes. The project has also contributed to the goal of maintaining and developing the competence and research capacity within Sweden. SKI will use FRAPCON-3 to evaluate safety aspects of fuel constructions from various fuel vendors. FRAPCON-3 will be used to generate input data to the computer code SCANAIR which is evaluated and reported within project number14.6-010185/01088.

The study of FRAPCON-3 concludes that the code is applicable to thermo-mechanical analyses of both BWR and PWR fuel rods under steady-state operational conditions, and to some extent also to slow power excursions. Rod average burnups up to 65 MWd/kg can be analysed. The report indicates however limitations in the applicability, primarily concerning $(U,Pu)O_2$ and $(U,Gd)O_2$ and analyses of pellet-clad mechanical interaction..

Project information:
Project manager: *Ingrid Töcksberg, Department of Reactor Technology, SKI*
Project number: *14.6-010960/01226*

SKI Report 02:29

Research

Evaluation of the FRAPCON-3 Computer Code

Lars Olof Jernkvist
Ali Massih

Quantum Technologies AB
Uppsala Science Park
SE-751 83 Uppsala
Sweden

March 2002

SKI Project Number 01226

LIST OF CONTENTS

Summary III

Sammanfattning IV

1 Introduction 1

2 FRAPCON-3 models 3

2.1 Modeling capability 3
2.1.1 Applicability 3
2.1.2 Geometrical representation 4
2.1.3 Time stepping 4
2.2 Thermal analysis 5
2.2.1 Fuel pellet 7
2.2.2 Pellet-to-clad gap 9
2.2.3 Clad tube 10
2.2.4 Clad oxide layer 11
2.2.5 Oxide-to-coolant interface 11
2.2.6 Coolant channel 12
2.2.7 Gas plenum 12
2.3 Mechanical analysis 13
2.3.1 Fuel pellet 13
2.3.2 Clad tube 14
2.3.3 Pellet-clad interaction 17
2.4 Rod internal gas analysis 19
2.4.1 Gas pressure calculation 19
2.4.2 Gas production and release 20
2.5 Clad waterside corrosion 21
2.5.1 Oxide growth 21
2.5.2 Clad hydrogen pickup 22
2.5.3 Crud growth 22

3 FRAPCON-3 interface 25

3.1 Input 25
3.2 Output 25
3.2.1 Tabulated data 26
3.2.2 Graphical output 26
3.3 Interface to FRAPTRAN 26

4 Code implementation and documentation 27

4.1 History 27
4.2 Code structure 27
4.3 Programming language and style 29
4.4 Code documentation 30

5 Code calibration and verification 31

5.1 Assessment data base 31
5.2 Fuel temperature 34
5.3 Fission gas release 36
5.4 Rod internal void volume 37
5.5 Clad corrosion 37
5.6 Clad deformation 38

6 Concluding remarks 39

7 References 41

Appendix A: FRAPCON-3 fuel thermal conductivity model 45

Appendix B: Halden fuel thermal conductivity model 49

Summary

The FRAPCON-3 computer code has been evaluated with respect to its applicability, modeling capability, user friendliness, source code structure and supporting experimental database. The code is intended for thermo-mechanical analyses of light water reactor nuclear fuel rods under steady-state operational conditions and moderate power excursions. It is applicable to both boiling- and pressurized water reactor fuel rods with UO_2 fuel, ranging up to about 65 MWd/kgU in rod average burnup.

The models and numerical methods in FRAPCON-3 are relatively simple, which makes the code transparent and also fairly easy to modify and extend for the user. The fundamental equations for heat transfer, structural analysis and fuel fission gas release are solved in one-dimensional (radial) and stationary (time-independent) form, and interaction between axial segments of the rod is confined to calculations of coolant axial flow and rod internal gas pressure.

The code is fairly easy to use; fuel rod design data and time histories of fuel rod power and coolant inlet conditions are input via a single text file, and the corresponding calculated variation with time of important fuel rod parameters are printed to a single output file in textual form. The results can also be presented in graphical form through an interface to the general graphics program `xmgr`. FRAPCON-3 also provides the possibility to export calculated results to the transient fuel rod analysis code FRAPTRAN, where the data can be used as burnup-dependent initial conditions to a postulated transient.

Most of the source code to FRAPCON-3 is written in Fortran-IV, which is an archaic, non-standard dialect of the Fortran programming language. Since Fortran-IV is not accepted by all compilers for the latest standard of the language, Fortran-95, there is a risk that the source code must be partly rewritten in the future.

Documentation of the code comprises (i) a general code description, which briefly presents models, computational methods and code structure, and (ii) an integral assessment report, which presents the performed code calibration with experimental data. In addition, there are two supporting documents related to the MATPRO materials properties package, which is extensively used in FRAPCON-3.

Our evaluation confirms the applicability of FRAPCON-3 to high burnup fuel rods, but also reveals weaknesses in several models. In particular, the models for UO_2 thermal conductivity degradation with increasing burnup, clad oxidation, creep, plasticity and irradiation-induced axial growth have been found to be less adequate. Suggestions for improvements to these models are pointed out in the report.

In conclusion, we believe that FRAPCON-3 constitutes a suitable computer code for steady-state fuel rod analysis, into which SKI can add new and improved models that satisfy their requirements.

Sammanfattning

Datorprogrammet FRAPCON-3 har utvärderats med avseende på användbarhet, modelleringsförmåga, användarvänlighet, källkodsstruktur och de experimentella data, på vilka programmets modeller är baserade. Programmet är avsett för analys av kärnbränslestavars termomekaniska beteende i lättvattenreaktorer vid såväl stationär drift som under måttliga effektuppgångar. Det kan användas för analys av UO_2-laddade bränslestavar med upp till 65 MWd/kgU i genomsnittlig stavutbränning, i både kok- och tryckvattenreaktorer.

De modeller och numeriska metoder som används i FRAPCON-3 är relativt enkla, vilket medför att programmet är lättöverskådligt och att det också tämligen enkelt kan modifieras och vidareutvecklas av användaren. De grundläggande ekvationerna för värmetransport, stavens mekaniska beteende och bränslets fissionsgasfrigörelse löses i endimensionell (radiell) och stationär (tidsoberoende) form, och koppling mellan olika axiella segment hos bränslestaven beaktas endast vid beräkning av kylmediets axiella flöde och det inre gastrycket i staven.

Programmet är relativt enkelt att använda; tillverkningsdata och effekthistorik för bränslestaven, liksom randvillkor i form av tidshistorier för kylmediets inloppstillstånd, ges som indata i en enkel textfil. Tidsutvecklingen av viktiga bränslestavparametrar beräknas från dessa data, och resultaten tabelleras i en separat utdatafil. Resultaten kan även presenteras i grafisk form via en koppling till det generella grafikprogrammet `xmgr`. FRACON-3 har också möjlighet att exportera beräkningsresultaten till programmet FRAPTRAN, vilket används för transientanalys av kärnbränslestavar. De exporterade resultaten kan därvid användas som utbränningsberoende begynnelsevillkor vid analys av en postulerad transient.

Merparten av källkoden till FRAPCON-3 är skriven i Fortran-IV, som är en föråldrad och icke standardiserad dialekt av programmeringsspråket Fortran. Då Fortran-IV ej accepteras av alla kompilatorer för den senaste standarden av språket, Fortran-95, finns det en framtida risk för att delar av källkoden måste skrivas om.

Programdokumentationen omfattar (i) en allmän programbeskrivning, vilken kortfattat beskriver modeller, beräkningsmetoder och källkodsstruktur, samt (ii) en övergripande utvärderingsrapport, vilken presenterar den kalibrering av programmet mot experimentella data som utförts. Dessutom finns ytterligare två dokument relaterade till materialdatabiblioteket MATPRO, vilket används flitigt i FRAPCON-3.

Vår utvärdering bekräftar att FRAPCON-3 kan användas för analys av bränslestavar vid hög utbränning, men avslöjar även svagheter i ett flertal modeller. I synnerhet modellen för urandioxidens försämrade termiska ledningsförmåga med ökande utbränning, samt modellerna för kapslingens oxidation, kryp, plasticitet och bestrålningsinducerade längdtillväxt har befunnits vara otillräckliga. Förslag till förbättringar av dessa modeller ges i rapporten.

Avslutningsvis anser vi att FRAPCON-3 utgör ett lämpligt beräkningsprogram för analys av bränslestavars beteende under stationär drift, i vilket SKI kan införa nya och förbättrade modeller som motsvarar deras behov.

1 Introduction

This is the first report in a series of three, in which the FRAPCON-3 computer code is evaluated with respect to its theoretical and numerical bases, modeling capability and supporting database. The FRAPCON-3 computer code is used for analyzing the thermo-mechanical behavior of a single light water reactor (LWR) fuel rod under normal, steady-state reactor operating conditions and mild transients. Based on prescribed time histories of fuel rod power and coolant inlet conditions, the code calculates the corresponding variation with time of fuel rod temperature, deformation, internal gas pressure and clad waterside corrosion, Berna *et al*. (1997). The code was developed for the United States Nuclear Regulatory Commission (NRC) by the Idaho National Engineering and Environmental Laboratory (INEEL) and Pacific Northwest National Laboratory (PNNL).

FRAPCON-3 is a descendent of FRAPCON-2, version 1.5. In comparison with this older version of the code, FRAPCON-3 has a simpler structure and extended capability to model high burnup fuel rods; FRAPCON-3 has been assessed and validated with respect to experimental data from 45 fuel rods, covering rod average burnups up to 74 MWd/kgU and peak linear heat generation rates up to 58 kW/m.

FRAPCON-3 is linked with a subset of the MATPRO material properties package, which has been modified to cater for high burnup effects. The MATPRO package is composed of modular subroutines that define materials properties for temperatures ranging from room temperature to temperatures above melting, Hagrman *et al.* (1981) and Lanning *et al.* (1997b).

The FRAPCON-3 code is one-dimensional in nature (radial), and interaction between axial segments of the rod is confined to calculations of coolant axial flow and rod internal gas pressure. The one-dimensional nature of the code is a significant drawback in analyses of pellet-cladding mechanical interaction, but makes the applied computational methods fairly simple and the code structure transparent. Moreover, the one-dimensional formulation brings execution times to a minimum. They are typical in the order of ten seconds on office-class personal computers, which makes the code feasible for probabilistic analyses.

The organization of this report is as follows:
In section 2, the FRAPCON-3 models and methods used for calculation of thermo-mechanical performance, internal gas behavior and clad corrosion are briefly reviewed. Section 3 presents an overview of input and output data to the code, and section 4 deals with code structure, implementation and documentation. Section 5 finally presents the data base used for code calibration and verification, and summarizes the most important findings from the hitherto performed code assessment.

2 FRAPCON-3 models

The FRAPCON-3 code is intended for analyses of light water reactor (LWR) fuel rod behavior, when changes of both power and boundary conditions are sufficiently slow for the term "steady-state" to apply. This includes situations such as long periods at constant power and slow power ramps that are typical of normal power reactor operations. The code calculates the variation with time of all significant fuel rod variables, including fuel and clad temperatures, clad stresses and strains, clad oxidation, fuel irradiation swelling, fuel densification, fission gas release, and rod internal gas pressure. In addition, the code is designed to generate initial conditions for transient fuel rod analysis by FRAPTRAN, the US NRC companion transient fuel rod analysis code, Cunningham *et al.* (2001).

In the sequel, a brief summary of general modeling capabilities and inherent limitations of the code is first presented. The summary is then followed by a more thorough review of the models and solution methods applied in FRAPCON-3.

2.1 Modeling capability

2.1.1 Applicability

FRAPCON-3 allows the thermo-mechanical behavior of both boiling water reactor (BWR) and pressurized water reactor (PWR) fuel rods to be analyzed. Material property data are taken from a slightly modified version of the MATPRO material properties package, which comprises models for UO_2 as well as mixed $(U,Gd)O_2$ and $(U,Pu)O_2$ fuel, and both Zircaloy-2 and Zircaloy-4 clad materials. However, the code calibration and verification has been performed only for UO_2 fuel, and FRAPCON-3 is currently not qualified for (U,PU) or (U,Gd) mixed oxide fuel; see section 5.1. To this end, it should also be noticed that the ability to predict cladding stresses and strains resulting from pellet-cladding mechanical interaction (PCMI) has not yet been thoroughly assessed. As currently configured, FRAPCON-3 is therefore not suited for analyses of clad deformation and failure due to PCMI.

As mentioned in the introduction, the application of FRAPCON-3 is restricted to simulations of steady-state operating conditions. Accordingly, the governing equations for fuel rod heat transfer and deformation are applied in their stationary (time-independent) form. Similarly, the fission gas release models are intended for steady-state operational conditions or slow power ramps, typical of normal power reactor operation. For simulation of fast power ramps and transients, the FRAPTRAN code must therefore be used, Cunningham *et al.* (2001).

FRAPCON-3 has been calibrated to experimental data from altogether 30 high burnup fuel rods with peak linear heat generation rates (LHGR) varying from 26 to 58 kW/m, fission gas release fractions from 1 to 30% and rod average burnups up to 74 MWd/kgU. The data base used for code assessment is restricted to normal reactor coolant conditions, and no calibration has been performed for cladding temperatures above 700 K.

2.1.2 Geometrical representation

In FRAPCON-3, the fuel rod geometry is represented by a stack of cylindrical fuel pellets, which are located symmetrically within a cylindrical clad tube. The clad tube is surrounded by a water/steam coolant, which has uniform properties along the clad periphery, as shown in figure 2.1. The considered configuration is thus axisymmetric.

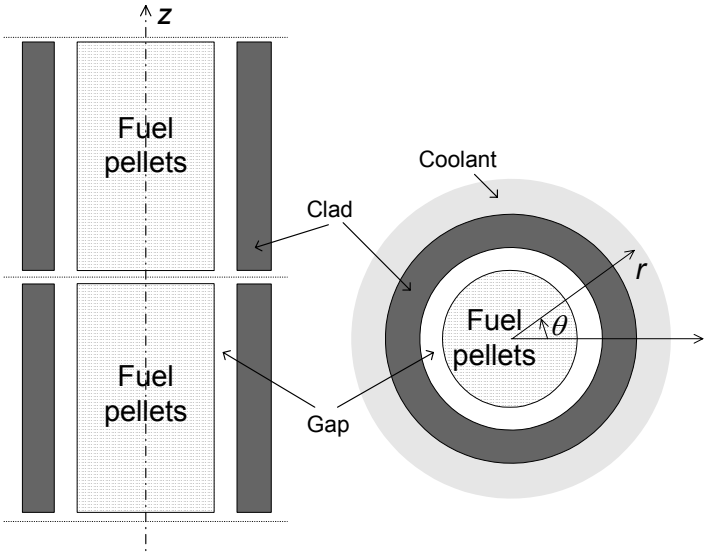

Figure 2.1: Geometrical representation of the fuel rod. Two axial segments of the rod are shown in the figure.

The active length of the fuel rod is divided into 1-18 axial segments, which are assumed to have identical dimensions and material properties, but different thermal loads. In addition, a gas plenum volume is assumed at the top of the fuel rod.

Fuel rod heat transfer and deformations are calculated for each axial segment individually, thus neglecting transfer of heat and mechanical forces between adjacent segments. This simplification, in combination with the assumed axial symmetry, makes the governing equations for heat transfer and deformations one-dimensional. Within each axial segment, the temperature and other variables are thus dependent on the radial coordinate only.

2.1.3 Time stepping

In FRAPCON-3, the stationary heat transfer equation and the equations of mechanical equilibrium are solved for a sequence of time steps. A maximum of 400 time steps can be used to define the fuel rod operating history. For each time step, the user has the possibility to prescribe

- Rod average power
- Coolant pressure
- Coolant inlet temperature
- Coolant mass flux

Moreover, the user can change the axial power shape from one predefined shape to another between each time step. A maximum of 20 axial power shapes can be predefined. The length of each time step must be defined by the user, and should be chosen in the range from 0.1 to 50 days. Other restrictions to the time step length are that changes in linear heat generation rate should not exceed 5 kW/m between time steps, and that the increase in local burnup should not exceed 2 MWd/kgU under the time step.

2.2 Thermal analysis

The thermal analysis in FRAPCON-3 comprises determination of the radially dependent temperature distribution in each axial segment of the fuel rod, as schematically depicted in figure 2.2.

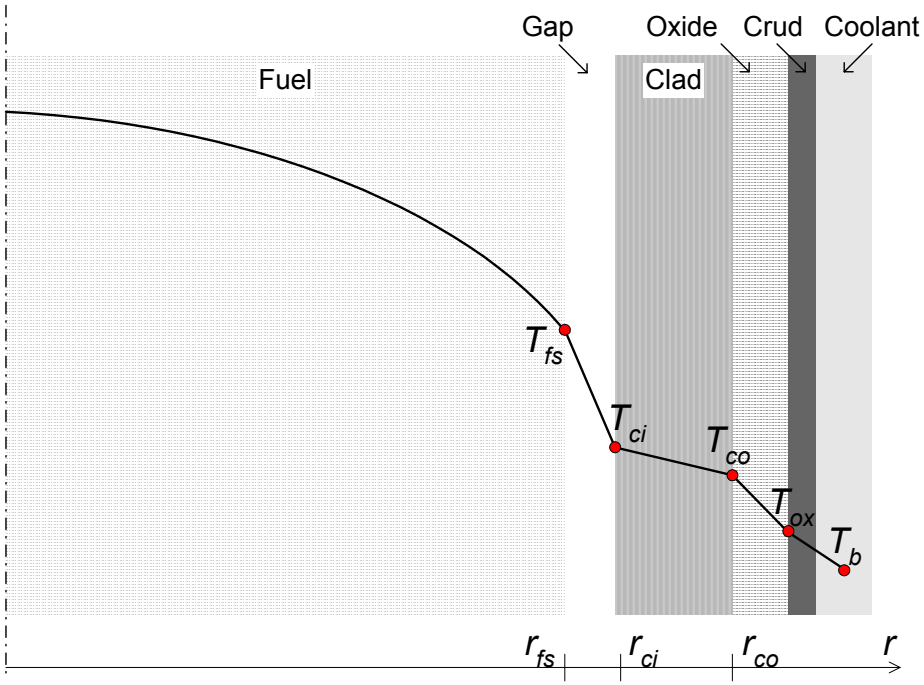

Figure 2.2: Schematic radial temperature profile in a specific axial segment of the rod.

Axial heat transport within fuel and clad is considered negligible relative to the radial direction, and axial heat transfer is therefore considered only in the coolant channel. The heat flux, $\vec{\phi}$, within the fuel rod can thus be written

$$\vec{\phi} = \phi \vec{e}_r , \tag{2.1}$$

where ϕ is the radial heat flux, and $\vec{e}_r$ is the radial unit vector. The radial heat flux is related to the applied linear heat generation rate (LHGR), $q'(z)$, through

$$\phi(r,z) = \frac{q'(z)}{2\pi r} , \tag{2.2}$$

where r and z are the radial and axial coordinates. It should be noticed, that $q'(z)$ is uniform within each axial segment, and that eq. (2.2) is valid only for stationary, steady-state conditions.

In the solids, *i.e.* in the fuel pellets, clad tube, and oxide layer, the radial heat flux is related to the temperature through Fourier's law of heat conduction,

$$\phi = -\lambda \frac{\partial T}{\partial r}, \tag{2.3}$$

where T is the temperature and λ is the thermal conductivity of the respective solid.

In FRAPCON-3, equations (2.1)-(2.3) are used in the time-independent heat balance equation, which in integral form is

$$\int_S \vec{\phi} \cdot d\vec{S} = \int_V \rho p \, dV . \tag{2.4}$$

Here, V and S denote the volume and boundary surface, respectively, of an arbitrary piece of the material, whereas ρ and p are the density and heat source per unit mass of the material. In FRAPCON-3, $p \neq 0$ only in the fuel pellet, *i.e*. heat generation in the clad tube as a result of gamma attenuation is neglected. The radial distribution of the heat source p is calculated by use of the TUBRNP power and burnup distribution model, developed by Lassman *et al.* (1994). This model is applicable to UO_2 and $(U,Pu)O_2$ fuel, but not to $(U,Gd)O_2$ fuel.

At the pellet-to-clad and oxide-to-coolant interfaces, the radial heat flux is calculated from Newton's law of cooling

$$\phi = H \Delta T , \tag{2.5}$$

where H is a parameter called the surface conductance or the surface heat transfer coefficient and ΔT is the temperature difference across the interface. Hence, with reference to figure 2.2, at the pellet-to-clad interface, $\Delta T = T_{fs} - T_{ci}$ and at the oxide-to-coolant interface, $\Delta T = T_{ox} - T_b$.

By use of equations (2.4) and (2.5), the radial temperature distribution in the fuel rod can be determined from the boundary conditions

$$\phi = 0 \text{ at } r = 0, \tag{2.6a}$$

$$T = T_b \text{ in the coolant.} \tag{2.6b}$$

The models and methods used for calculation of the radial temperature distribution are described in the sequel, beginning with the fuel pellets and ending with the coolant channel. In practice, however, the calculations are performed in the opposite order: First, the coolant bulk temperature variation along the fuel rod is calculated directly from the supplied input. Next, the calculation proceeds in the inward radial direction for each axial segment individually. The increase in temperature when passing from the coolant to the oxide layer and further through the clad metal and pellet-to-clad gap can be calculated by means of fairly simple analytical expressions. However, from the pellet surface and inwards, the radial temperature distribution must be calculated by use of numerical methods.

2.2.1 Fuel pellet

One of the major differences between FRAPCON-3 and its predecessors concerns the fuel pellet heat conduction modeling. The current model is based upon a finite difference solution method to the heat conduction equations, which is also used in RELAP5 and FRAPTRAN, Cunningham *et al*. (2001). In FRAPCON-2, a method of weighted residuals was used, Berna *et al*. (1980). The new model was introduced in order to provide consistency with FRAPTRAN, and also to allow accurate calculation of temperatures in high burnup fuels by a better representation of the fuel pellet rim region.

In the new FRAPCON-3 model, the radial fuel pellet temperature distribution is determined by applying the heat balance equation (2.4) to a number of annular volumes; see figure 2.3. Thinner annuli are used close to the pellet surface (rim region) in order to resolve the steep radial gradient in burnup and heat generation rate that is characteristic for this position in high burnup fuel. The spatial discretization is fully consistent with the new radial power and burnup distribution model TUBRNP, which has also been incorporated in FRAPCON-3 , (Lassman *et al*., 1994).

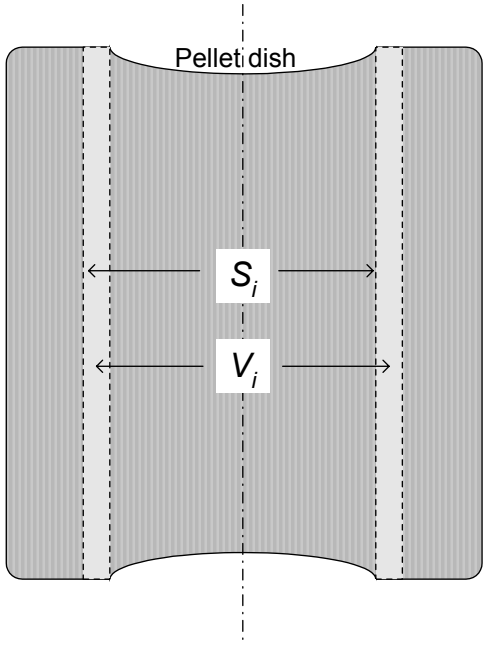

Figure 2.3: Discretization of the fuel pellets into annuli. The figure shows the i:th annulus, with volume V_i and surface S_i.

In each annulus, the temperature, material properties and heat source are assumed to be uniform. The discretization leads to a tridiagonal system of equations in the unknown temperatures, which given the boundary condition in eq. (2.6a) and a known fuel pellet surface temperature can be efficiently solved by direct back-substitution.

The fuel thermal conductivity, λ_{fuel}, is correlated to the local temperature, burnup, Gd/Pu content and porosity through a model proposed by Lucuta *et al.* (1996)

$$\lambda_{fuel} = \lambda_0 F_D F_P F_M F_R . \tag{2.7}$$

Here, λ_0 is the conductivity of unirradiated, fully dense fuel, as given by Harding and Martin (1989), F_D and F_P are burnup dependent corrections for dissolved and precipitated fission products in the fuel matrix, F_M is a correction factor for fuel porosity, and F_R is a temperature dependent compensation factor for irradiation effects. The model in eq. (2.7) is fully described in appendix A.

Comment:

The predicted thermal conductivity for UO_2 fuel with 4% porosity (0.96 of theoretical density) is plotted in figure 2.4 as a function of temperature and burnup. Evidently, the conductivity degradation with increasing fuel burnup is most pronounced for temperatures below 1500 K. In figure 2.5, the fuel conductivity model used in FRAPCON-3 is compared with an empirical model, which has been derived from in-reactor temperature measurements on high burnup fuel at the Halden experimental reactor, Vitanza (1995). The Halden model is described in appendix B.

Figure 2.5 shows the relative degradation of thermal conductivity with increasing burnup, *i.e.* the product $F_D F_P$ in eq. (2.7), for UO_2 fuel with 4% porosity. It is interesting to note, that the model applied in FRAPCON-3 predicts a less severe thermal conductivity degradation than the model based on Halden reactor experimental data. Supported by figure 2.5 and the conclusions drawn from assessment of fuel temperature predictions in section 5.2, it is most likely that the FRAPCON-3 model underestimates the effect of thermal conductivity degradation with increasing burnup.

According to the model in eq. (2.7), the thermal conductivity actually increases slightly with increasing burnup in the range from 0 to 5 MWd/kgU for T=1500 K. This is due to an alleged beneficial effect of precipitated fission products, having much better conductivity than UO_2, on the overall conductivity of the material. The factor F_P in eq. (2.7) is therefore larger than unity.

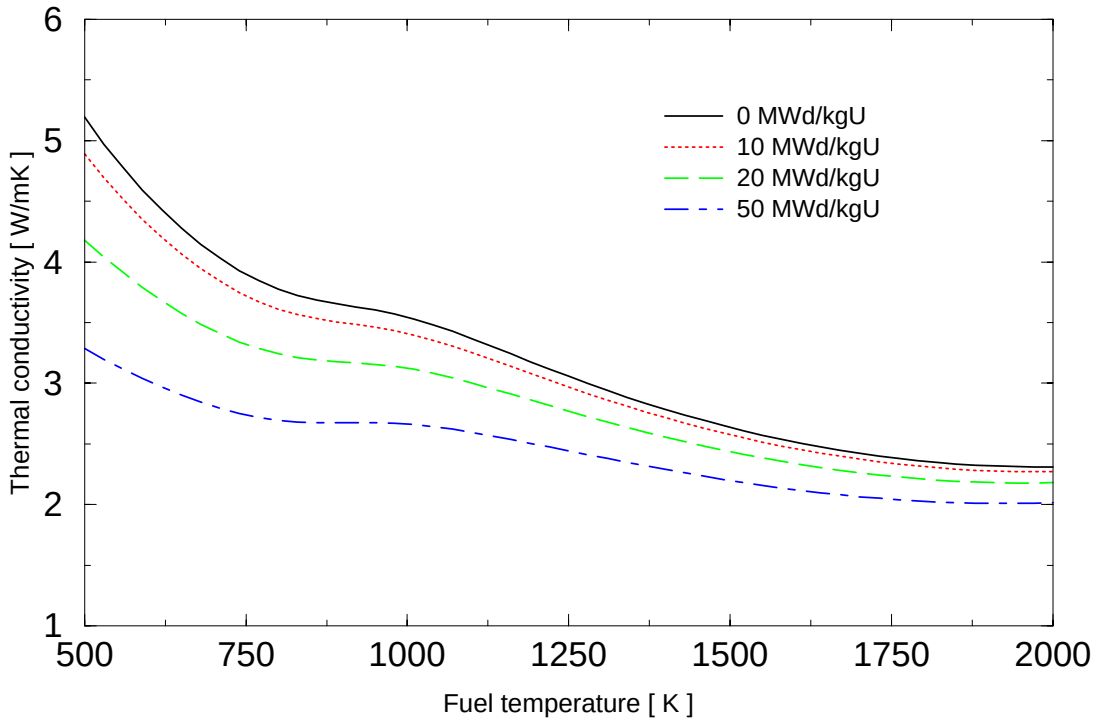

Figure 2.4: Thermal conductivity of irradiated UO_2 fuel with 4% porosity, as calculated with the FRAPCON-3 conductivity model in eq. (2.7).

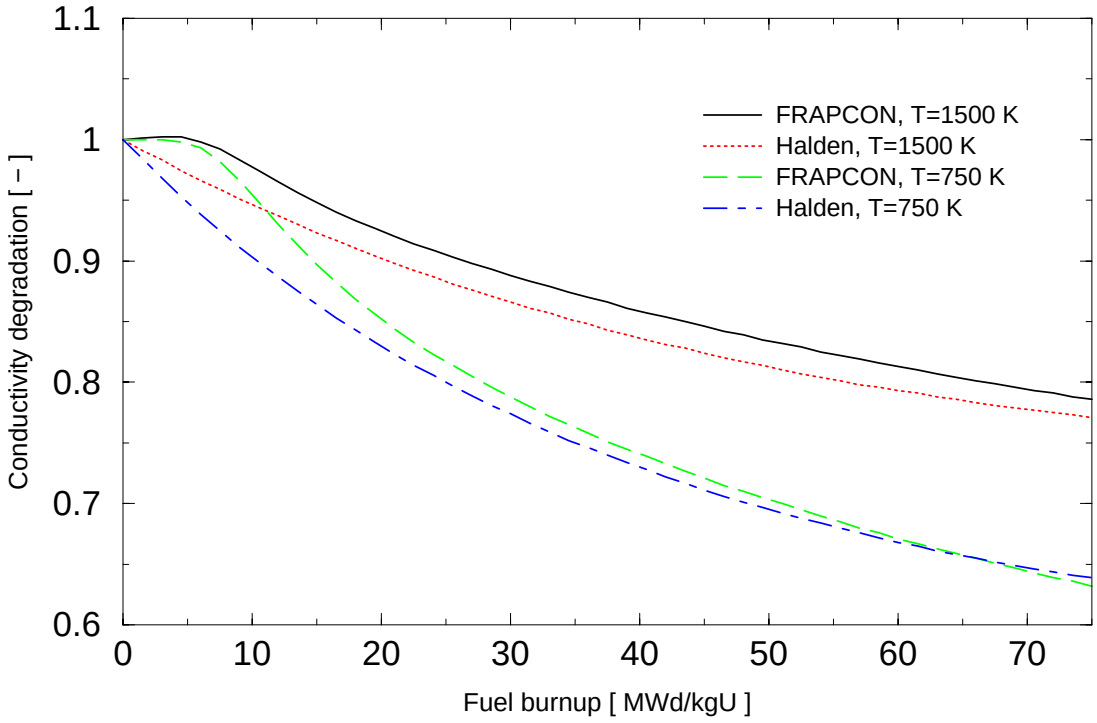

Figure 2.5: Thermal conductivity degradation of irradiated UO_2 fuel with 4% porosity, as calculated with the FRAPCON-3 and Halden reactor models, respectively.

2.2.2 Pellet-to-clad gap

The model for heat transfer across the pellet-to-clad gap considers contributions from three different heat transport mechanisms

- Conduction through the gap gas
- Pellet-to-clad radiation
- Pellet-to-clad contact conduction

The heat transfer coefficient H in eq. (2.5) can thus for the gap be written as

$$H_{gap} = H_{gc} + H_r + H_{cc}, \tag{2.8}$$

where H_{gc}, H_r and H_{cc} are the heat transfer coefficients related to gas conduction, radiation and contact conduction. These coefficients are obtained from mechanistic models, and the temperature drop across the pellet-to-clad gap in each axial segment is calculated from the prescribed liner heat generation rate, q', by combining eqs. (2.2) and (2.5)

$$T_{fs} - T_{ci} = \frac{q'}{\pi(r_{fs} + r_{ci})H_{gap}}, \tag{2.9}$$

where r_{fs} and r_{ci} are the fuel surface and clad inner radii in the axial segment under consideration.

The heat transfer coefficient related to gas conduction is calculated from a model, in which H_{gc} is dependent primarily on the pellet-clad gap size and on the temperature and composition of the gas, Beyer *et al.* (1975). The heat transfer coefficient related to radiation, H_r, is calculated from the pellet and clad surface temperatures through the Stefan-Boltzmann law, (Reif, 1965), whereas the contact conductance H_{cc} is correlated to the pellet-clad contact pressure through a modified form of the widely used model by Todreas and Jacobs, (1973).

Comment:
The pellet-to-clad gap heat transfer is significantly influenced by the gap size (open gap) and contact pressure (closed gap). To this end, it should be noticed that the gap size used in calculation of H_{gc} is an effective gap size, in which radial relocation of fuel fragments is considered. The relocation model, as described in section 2.3.1, is merely an empirical correlation for calculating an effective gap size that provides best-estimate predictions of fuel temperatures in FRAPCON-3. When the pellet-clad gap closes, 50% of the calculated fuel relocation is assumed to be reversible. This compression is assumed to take place under compression from the contacting cladding, without any resisting forces from the fragmented fuel. The remaining relocation is completely irrecoverable, irrespective of the pellet-clad contact pressure. Hence, only half of the fuel radial expansion calculated by the relocation model in section 2.3.1 is considered in calculations of the pellet-clad contact pressure.

A comment should also be made on the gas composition in the pellet-clad gap. In FRAPCON-3, instantaneous and complete mixing of released fission gases with the <u>*total*</u> internal gas volume is assumed. Fission gas released from the fuel at a certain axial position is thus assumed to mix instantaneously with gas residing in the pellet-clad gap along the entire fuel rod and in the fuel rod plenum volume.

2.2.3 Clad tube

The temperature drop from the inside ($r=r_{ci}$) to the outside ($r=r_{co}$) of the clad tube is calculated for each axial segment through an analytical solution for steady state radial heat conduction through a cylinder

$$T_{ci} - T_{co} = \frac{q'(z)\ln(r_{co}/r_{ci})}{2\pi\lambda_{clad}} , \qquad (2.10)$$

where T_{ci} and T_{co} are the clad inner and outer temperatures, as shown in figure 2.2.

Comment:
The expression in eq. (2.10) constitutes an exact solution, only if

1) Steady-state conditions prevail
2) No heat is generated in the clad material
3) The thermal conductivity λ_{clad} is uniform across the clad wall

Fulfillment of condition 2) is obtained by neglecting heat generation through gamma attenuation in the clad. Condition 3) is only approximately satisfied, since the clad thermal conductivity is dependent on temperature, Hagrman *et al.* (1981). In FRAPCON-3, a uniform thermal conductivity, corresponding to the clad average temperature, is used in eq. (2.10).

2.2.4 Clad oxide layer

The temperature drop across the oxide layer can be calculated through the same analytical solution as is used for the clad tube in eq. (2.10). However, since the oxide layer is thin, the logarithm can be approximated with the first term of a series expansion. The temperature drop across the clad oxide layer at axial elevation z is thereby calculated from

$$T_{co} - T_{ox} = \frac{q'(z)}{2\pi\lambda_{ox}} \frac{\delta_{ox}(z)}{r_{co}}, \tag{2.11}$$

where T_{ox} is the oxide surface temperature, as shown in figure 2.2, λ_{ox} is the oxide thermal conductivity, calculated from the clad temperature through a correlation presented in section 2.5.1, and δ_{ox} is the oxide layer thickness. For each axial segment, the oxide layer growth is modeled by the correlations presented in section 2.5.1.

2.2.5 Oxide-to-coolant interface

The temperature of the oxide surface, T_{ox}, at elevation z is taken as the minimum of

$$T_{ox}(z) = T_b(z) + \Delta T_{cr}(z) + \Delta T_{fc}(z) \quad \text{or} \tag{2.12}$$

$$T_{ox}(z) = T_{sat} + \Delta T_{nb}(z). \tag{2.13}$$

Here, T_b and T_{sat} are the coolant bulk and saturation temperatures, ΔT_{cr}, ΔT_{fc} and ΔT_{nb} are temperature drops related to the crud layer, forced convection film boiling and nucleate boiling heat transfer. The choice of the minimum value of eq. (2.12) or (2.13) is a simple means of deciding whether heat is transferred from the clad surface to the coolant by forced convection or nucleate boiling. It also provides a smooth numerical transition from forced convection to nucleate boiling, thereby avoiding convergence problems. The temperature drop across the crud layer (if any) is calculated through

$$\Delta T_{cr}(z) = \frac{q'(z)}{2\pi\lambda_{crud}} \frac{\delta_{crud}}{r_{co}}, \tag{2.14}$$

where δ_{crud} and λ_{crud} is the crud layer thickness and thermal conductivity, respectively. The crud thickness is either provided as a constant value by the user, or calculated through the simple growth laws presented in section 2.5.3.

For forced convection heat transfer, as given by eq. (2.12), the temperature drop ΔT_{fc} across the coolant film layer is calculated through the Dittus-Boelter correlation. For nucleate boiling heat transfer, as given by eq. (2.13), the temperature drop ΔT_{nb} at the oxide surface is calculated through the Jens-Lottes correlation.

Comment:

Under nucleate boiling, the coolant is assumed to boil through the crud layer, and the temperature drop across the crud layer is therefore not explicitly considered.

2.2.6 Coolant channel

The coolant temperature is calculated by use of a one-dimensional enthalpy raise model. The governing equations are thus the conservation of mass and the conservation of energy in the axial (z) flow direction. Conservation of momentum is not considered, and the coolant pressure is therefore modeled as uniform along the fuel rod.

From the governing equations, the coolant bulk temperature, T_b, at axial position z can be calculated from

$$T_b(z) = T_{inlet} + \int_0^z \frac{2q'(z)}{\pi G C_p D_e r_{co}} dz , \tag{2.15}$$

where T_{inlet} is the coolant inlet temperature, G and C_p are the coolant mass flux and heat capacity, and D_e is the coolant channel heated diameter, calculated from

$$D_e = \frac{2(\Delta^2 - \pi r_{co}^2)}{\pi r_{co}} , \tag{2.16}$$

where r_{co} is the clad outer radius and Δ is the rod-to-rod distance (pitch) in the fuel assembly. The coolant inlet temperature and mass flux are prescribed functions of time, and supplied by the user as input to FRAPCON-3. Since the same is true for the axial power profile $q'(z)$, the coolant bulk temperature along the fuel rod can be calculated directly from input through eq. (2.15).

2.2.7 Gas plenum

The plenum gas temperature has importance to calculations of the rod internal gas pressure. In FRAPCON-3, the plenum gas temperature is calculated through an empirical model, which considers heat supply to the gas from the top of the pellet stack and from the gamma heated hold down spring within the plenum. The heat supply is balanced by heat removal from the gas to the coolant via the plenum clad walls.

2.3 Mechanical analysis

The main objective of the mechanical analyses in FRAPCON-3 is to calculate the fuel and clad deformations, which are necessary for accurate determination of the rod internal gas pressure and the pellet-to-clad heat transfer.

Mechanical analyses in FRAPCON-3 are performed by use of rather simple models, taken from the FRACAS-I subcode, Bohn (1977). The models are based on small-strain theory, and analyses are thus restricted to small deformations. The fuel is treated as a completely rigid material, which swells or shrinks in stress-free condition due to thermal expansion, swelling and densification. The fuel deformation is thus affected neither by restricting forces from the clad tube, nor by internal stresses in the fuel material.

2.3.1 Fuel pellet

The assumptions made with respect to fuel deformation in FRAPCON-3 are that no pellet deformation is induced by fuel-cladding contact stresses or internal thermal stresses, and that free-ring expansion applies. Each fuel annulus in figure 2.3 is thus assumed to expand without restraint from other annuli, and the total expansion is the sum of the expansions of all annuli. The deformation mechanisms considered in the fuel are

- Thermal expansion
- Athermal swelling from accumulation of solid fission products
- Densification
- Fragment relocation (only in the radial direction)

The radial deformation of the pellet due to thermal expansion, irradiation induced swelling and densification is calculated with the free-ring expansion model. In this model, the governing equation for the fuel pellet surface radial displacement is

$$u(r = r_{fs}) \;=\; \sum_{i=1}^{N} \Delta r_i \left[1 + \alpha_T (T_i - T_{ref}) + \varepsilon_i^d + \varepsilon_i^s \right] \;-\; r_{fs}\,, \qquad (2.17)$$

where subscript i alludes to the i:th fuel annulus with thickness Δr_i, and N is the total number of annuli. The coefficients of thermal expansion, α_T, and the strains from fuel densification, ε_i^d , are calculated through correlations in the original MATPRO package, Hagrman *et al*. (1981). The strains associated with solid fission product swelling, ε_i^s , are calculated from a new model, which has been assessed against high-burnup fuel density data, Lanning *et al.* (1997b).

Axial deformation of the total fuel stack takes into account the thermal, densification, and swelling strains at each axial node. The calculation proceeds differently for flat-ended versus dished pellets. For flat-ended pellets, the volume-averaged ring axial deformation is calculated for each axial segment, and these are summed to find the total stack deformation. For dished pellets, the axial deformation of the "maximum ring" (the ring with the maximum deformed length) per axial segment is found, and these "maximum ring" deformations are summed to find the total deformation. Typically, the "maximum ring" is the annulus just outside the pellet dish, because the axial expansion of the rings within this position is fully accommodated by the dish. Figure 2.3 shows the typical position of the maximum ring.

Relocation of fuel fragments is considered only in the radial direction. The relocation model originates from the GT2R2 code, Cunningham and Beyer (1984), but has been modified in order to provide a best estimate prediction of fuel temperatures in FRAPCON-3, Lanning *et al.* (1997b). The model is thus empirical, and correlates the fuel radial relocation, *i.e.* the apparent increase of fuel radius, to the fuel rod as-fabricated gap size, burnup and current linear heat generation rate. The radial relocation constitutes an additional contribution to the fuel radial expansion in eq. (2.17).

The relocated fuel radius is used in calculations of the pellet-to-clad heat transfer coefficients and also in determination of the rod internal free volume. However, in calculation of the pellet-clad contact pressure, only 50% of the radial relocation is considered. The remaining part of the relocation is assumed to be recovered without any resisting forces under compression from the surrounding clad tube, and therefore does not contribute to the pellet-clad mechanical interaction.

Comment:
The fuel radial relocation at any point in time is in FRAPCON-3 correlated to the <u>current</u> linear heat generation rate. In reality, fuel fragment relocation is a time-dependent phenomenon, which is affected by fuel creep and fragment movements under influence of flow-induced vibrations in the fuel rod. The radial relocation should therefore be modeled with consideration not only of the current power, but also of the preceding power history. The relocation model in FRAPCON-3 is thus restricted to applications, in which rod power varies slowly and smoothly over time.

2.3.2 Clad tube

The cladding is in FRAPCON-3 treated as a thin-walled axisymmetric tube with uniform temperature across the wall thickness. Moreover, both loading and deformation are assumed to be axisymmetric, and shear stresses and strains are neglected. The deformation mechanisms considered in the clad tube are

- Elasticity
- Thermal expansion
- Irradiation-induced axial growth
- Time-independent plasticity
- Creep

Except for the models for thermal expansion and irradiation-induced growth, the clad material is treated as isotropic. The texture induced anisotropy in elasticity, plasticity and creep is thus neglected, and the incremental deformations in the radial-, tangential- and axial direction (r, θ, z) under a specific time step can be expressed in terms of total strain increments $d\varepsilon_r$, $d\varepsilon_\theta$ and $d\varepsilon_z$ through

$$d\varepsilon_r = -\frac{\nu}{E}\left(d\sigma_\theta + d\sigma_z \right) + d\varepsilon_r^p + d\varepsilon_r^c + \alpha_r dT , \tag{2.18}$$

$$d\varepsilon_\theta = \frac{1}{E}\left(d\sigma_\theta - \nu d\sigma_z \right) + d\varepsilon_\theta^p + d\varepsilon_\theta^c + \alpha_\theta dT , \tag{2.19}$$

$$d\varepsilon_z = \frac{1}{E}\left(d\sigma_z - \nu d\sigma_\theta \right) + d\varepsilon_z^p + d\varepsilon_z^c + \alpha_z dT + d\varepsilon_z^g . \tag{2.20}$$

Here, E and ν are Young's modulus and Poisson's ratio, and dT the temperature increment during the time step. Superscripts p, c and g denote strain increments from plasticity, creep and irradiation-induced growth. The radial stress component does not appear in eqs. (2-18)-(2.20), since it is neglected in the thin-shell approximation of the clad tube. The material models used for the clad deformation mechanisms in FRAPCON-3 are briefly described below.

Elasticity and thermal expansion:
Young's modulus, Poisson's ratio and the coefficients of thermal expansion for the clad material are calculated through correlations in the original MATPRO package, Hagrman *et al*. (1981).

Irradiation-induced axial growth:
The axial strain due to irradiation effects in Zircaloy is correlated to the fast neutron fluence, Φ (> 1 MeV), through

$$\varepsilon_z^g \propto \Phi^{0.845} \tag{2.21}$$

The relation in eq. (2.21) is due to Franklin (1982). The growth strain is calculated at each axial segment, using the local fluences of fast neutrons. The axial elongations of all segments are then summed to obtain the total rod growth, which is of interest in determination of the rod free volume.

Time-independent plasticity:
The clad plastic strain increments are calculated from an isotropic strain hardening material model in MATPRO, which has been modified to account for the effects of hydriding in severely corroded clad materials, Lanning *et al.* (1997b). The von Mises isotropic yield criterion and associated flow rule are used for calculation of $d\varepsilon_r^p$, $d\varepsilon_\theta^p$ and $d\varepsilon_z^p$ for any given state of stress in the material. The method of successive elastic solutions is used for solving the non-linear equations, which are obtained as a result of plastic deformation, Mendelson (1968).

Comment:
The methods applied in FRAPCON-3 for calculation of clad plastic deformation have shown to give highly erroneous results under conditions of pellet-clad mechanical interaction, Jernkvist and Manngård (2002).

Creep:
The creep strain increments are calculated from a strain hardening creep model, in which the creep strain rate is correlated to stress, temperature, fast neutron flux and accumulated creep strain. The dependencies on time and stress are derived from in-reactor creep rate data from Ibrahim (1973), the flux dependence is based on Ross-Ross and Hunt (1968), and the temperature dependence is derived from Fidleris (1976). The same model is applied to both BWR and PWR conditions, and no distinction is made between materials with different chemical composition or heat treatment.

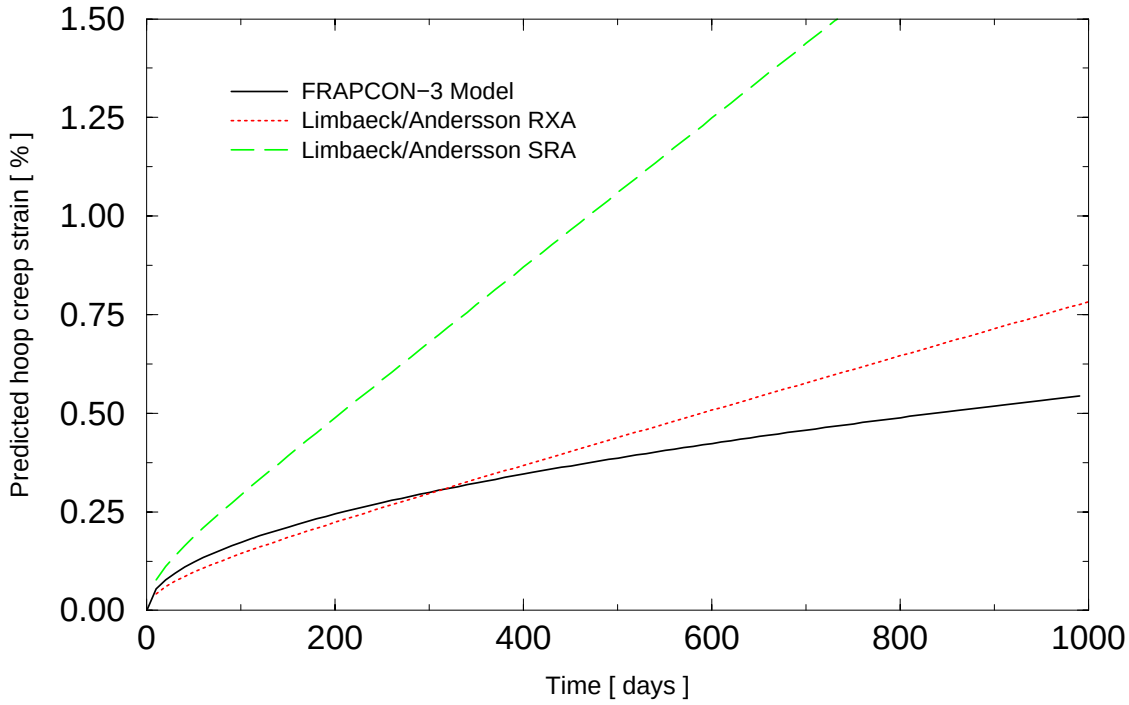

Figure 2.6: Predicted clad creep under typical PWR operating conditions; temperature 340 °C, tangential stress 80 MPa and fast (> 1 MeV) neutron flux $4 \cdot 10^{17}$ n/(m^{2}s).

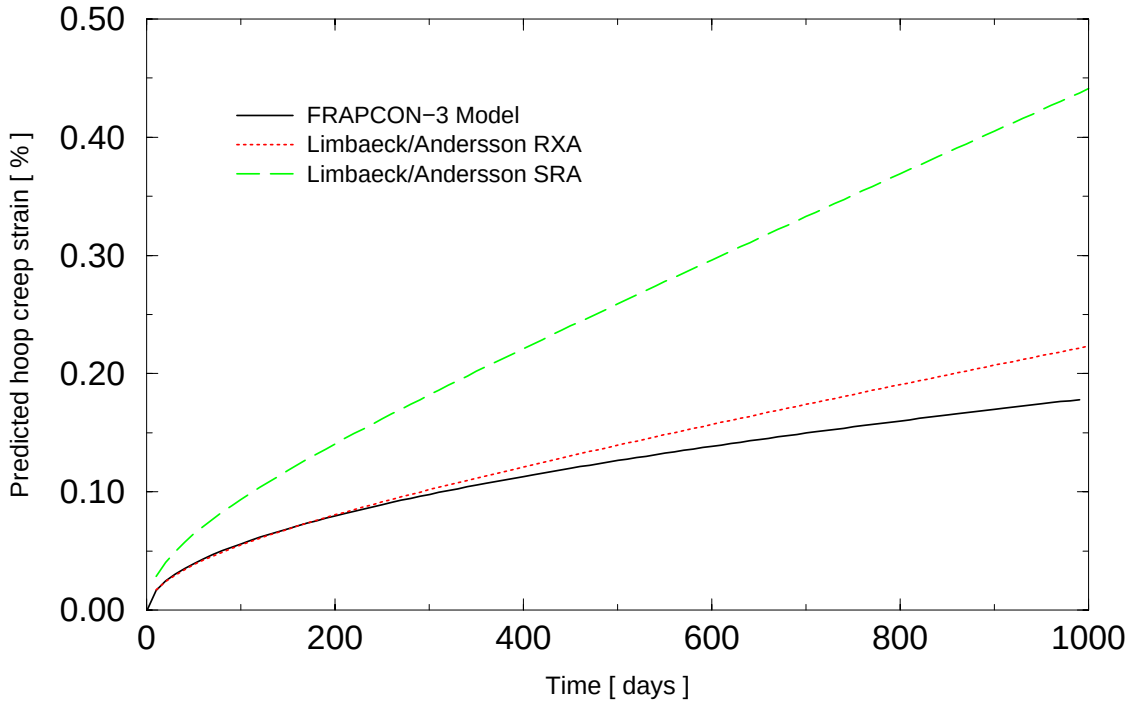

Figure 2.7: Predicted clad creep under typical BWR operating conditions; temperature 310 °C, tangential stress 40 MPa and fast (> 1 MeV) neutron flux $4 \cdot 10^{17}$ n/(m^{2}s).

Comment:
The experimental data, upon which the creep model is based, are for Zircaloy-2 materials in BWR environments only, which implies that the creep model has weak support for PWR applications. Moreover, the underlying experimental data to the model seem to be fairly old, and their relevance to current clad materials is questionable.

The hoop creep strain predicted by FRAPCON-3 under constant stress, temperature and fast neutron flux is shown in figures 2.6 and 2.7. The predictions from a recent creep model by Limbäck and Andersson (1996) are also shown for comparison. Their model is based on testing of clad materials fabricated by Sandvik, and a distinction is made between materials with different heat treatments. Recrystallization annealed (RXA) clad materials are used predominantly in BWR's, whereas stress relief annealed materials (SRA) are normally used in PWR's.

The FRAPCON-3 predictions are close to those obtained for the RXA material in the Limbäck/Andersson model, which confirms the suspicion that the creep model used in FRAPCON-3 is applicable primarily to BWR conditions.

2.3.3 Pellet-clad interaction

In mechanical analyses of the fuel rod behavior, the deformation of the clad tube may be affected by contact forces from the expanding fuel pellets, but the opposite is not true; as a result of the rigid pellet model in FRAPCON-3, the deformation of the fuel pellets is always independent of the pellet-clad contact pressure.

The mechanical analyses are performed for each axial segment of the fuel rod independently, and each segment may have an open or closed pellet-clad gap, as shown in figure 2.8. The computation of clad stresses and strains for these two gap configurations are described below.

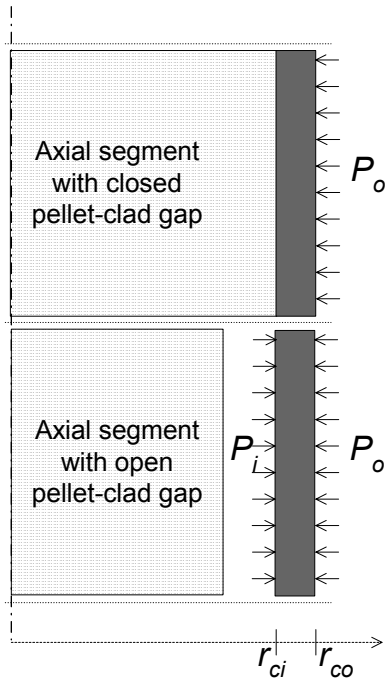

Figure 2.8: Fuel rod axial segments with open and closed pellet-clad gaps.

Open gap:
When the gap is open, the loads imposed on the clad tube are due solely to the rod internal pressure P_i and the coolant pressure P_o. The clad stresses in the tangential and axial directions are in this case directly obtained from the equations of equilibrium for a thin cylindrical shell (boiler formulas)

$$\sigma_\theta = \frac{r_{ci}P_i - r_{co}P_o}{r_{co} - r_{ci}}, \tag{2.22}$$

$$\sigma_z = \frac{r_{ci}^2P_i - r_{co}^2P_o}{r_{co}^2 - r_{ci}^2}, \tag{2.23}$$

where r_{ci} and r_{co} are the inner and outer radii of the clad tube. The radial stress component, σ_r, is neglected, since its magnitude is much less than the circumferential and axial stresses.

Together with the calculated clad temperature, the stresses in eqs. (2.22) and (2.23) are sufficient to calculate the resulting increments of strain through eqs. (2.18)-(2.20). If the effective von Mises stress exceeds the material yield stress in the considered time step, time-independent plastic deformation takes place, and the calculation of strain increments needs to be performed iteratively.

Closed gap:
When the gap in an axial segment closes, the following assumptions are made about the clad deformations:

1) The clad inner surface incremental displacement in the radial direction coincides with that of the pellet surface
2) The increment in clad axial strain coincides with that of the contacting fuel pellets

These two conditions thus imply that, from the point in time where the gap closes, fuel and clad are perfectly stuck within the axial segment. Moreover, as shown in section 2.3.1, the pellet deformation is dictated by the fuel temperature distribution (thermal expansion) and burnup (densification and swelling). When the gap is closed, the clad tube thus constitute a cylindrical shell, for which the increments of radial displacement of the inside surface and axial strain are prescribed. Here, the clad stresses cannot be computed directly, since the pellet-clad contact pressure at the clad inner surface must be determined as part of the solution.

Comment:
In FRAPCON-3, closure of the pellet-clad gap in one axial segment only affects the clad stress state in that very segment; as shown in figure 2.8, adjacent segments with open pellet-clad gaps are not affected by the PCMI and they thus experience the axial stress given by eq. (2.23).

In reality, one usually has a situation as shown in figure 2.9. When the pellet-clad gap closes in an axial segment, the clad tube in all segments below the contact point will experience the same axial tensile forces when the fuel pellet column expands. Only the segments above the contact point are unaffected by the PCMI. A much more elaborate computational approach is needed to consider this interaction of axial contact forces between fuel rod axial segments, since mechanical analyses for the axial segments can not be performed independently.

The current treatment of pellet-clad interaction in FRAPCON-3 is thus somewhat simplistic. It may lead to underprediction of rod axial growth in high burnup fuel rods; a phenomenon which is known to be affected by PCMI-induced axial forces in the clad material.

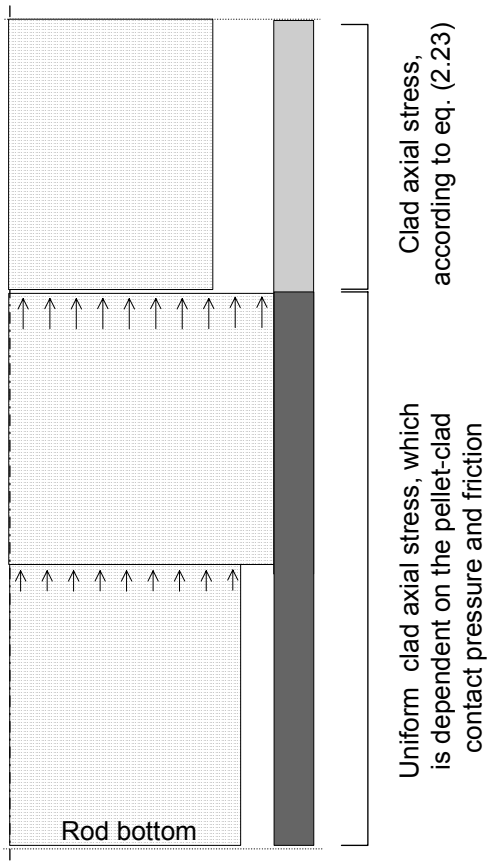

Figure 2.9: Transfer of axial clad forces to axial segments below the point of pellet-clad mechanical interaction. This effect is <u>not</u> considered in FRAPCON-3.

2.4 Rod internal gas analysis

The calculation of rod internal gas pressure is based on calculated temperatures, deformations and amount of gas released from the fuel. The models and methods applied in the analysis are presented in the sequel.

2.4.1 Gas pressure calculation

The rod internal gas pressure is calculated from the perfect gas law. The law is applied to a multiple region volume, in which all regions are assumed to have the same pressure, but different gas temperatures. The rod internal pressure, P_i, is

$$P_i = \frac{MR}{\frac{V_p}{T_p} + \sum_{i=1}^{N}\left(\frac{V_g^i}{T_g^i} + \frac{V_{ch}^i}{T_{ch}^i} + \frac{V_{cr}^i}{T_{cr}^i} + \frac{V_{dish}^i}{T_{dish}^i} + \frac{V_{por}^i}{T_{por}^i} + \frac{V_r^i}{T_r^i} + \frac{V_{\text{int}}^i}{T_{\text{int}}^i}\right)} \quad (2.24)$$

where M is the total amount of gas in moles, R is the universal gas constant, V_p and T_p are the plenum volume and temperature, N is the number of axial segments, and the following partial volumes and temperatures refer to the i:th axial segment

V_g^i , T_g^i	Pellet-to-clad gap volume and temperature
V_{ch}^i , T_{ch}^i	Pellet central hole volume and temperature
V_{cr}^i , T_{cr}^i	Pellet crack volume and temperature
V_{dish}^i , T_{dish}^i	Pellet dish volume and temperature
V_{por}^i , T_{por}^i	Pellet open porosity volume and temperature
V_r^i , T_r^i	Gap surface roughness volume and temperature
V_{int}^i , T_{int}^i	Pellet-to-pellet interface volume and temperature

These quantities are thus calculated for each axial segment individually, based on the current temperature distribution and fuel rod deformations.

2.4.2 Gas production and release

In FRAPCON-3, the total amount of gas in the fuel rod is calculated with consideration of released gaseous fission products (Xe, He, Kr) and nitrogen. The nitrogen is not a fission product, but is trapped in the fuel lattice during fuel fabrication and subsequently released under operation.

The amount of fission gas produced in the i:th axial segment of the rod is proportional to the segment's average burnup Bu^i and fuel volume V_{fuel}^i

$$M_{fiss}^i \propto V_{fuel}^i \left(Y_{Xe} + Y_{He} + Y_{Kr} \right) Bu^i . \tag{2.25}$$

Here, Y_{Xe}, Y_{He} and Y_{Kr} denote the fission yield (number of gas atoms produced per fission) of xenon, helium and krypton. Only a fraction of the produced fission gas in eq. (2.25) is released from the fuel to the rod free volume, where it contributes to the build up of the rod internal gas pressure. There are two optional models for fission gas release (FGR) in FRAPCON-3; the ANS-5.4 model (American Nuclear Society, 1982) and a modification of the model proposed by Forsberg and Massih (1985). Earlier versions of FRAPCON contained several other models.

2.4.2.1 ANS-5.4 fission gas release model

The ANS-5.4 model is intended for fission gas release under steady-state operational conditions. The model is divided into two main parts, one for release of stable isotopes and the other for release of short-lived isotopes. There are thermal and athermal models for both the stable and unstable fission products. The thermal model is based on diffusion of gas through the fuel matrix directly to the fuel surface, where the gas is released.

2.4.2.2 Forsberg/Massih fission gas release model

The model proposed by Forsberg and Massih is intended for fission gas release under steady-state operational conditions and mild transients. The model accounts for both thermal and athermal fission gas release, but only stable isotopes are considered.

In contrast to the ANS-5.4 model, the model by Forsberg and Massih accounts for the two-stage nature of thermal fission gas release. In the first stage, the produced fission gases diffuse to the grain boundaries, where they precipitate into intergranular bubbles. In the second stage, saturation of the grain boundary bubbles occurs and the accumulated gas is released from the fuel. The release upon grain boundary saturation is modeled as a fast mechanism, which is well in line with experimental observations of grain boundary gas release taking place within minutes or hours during power excursions. The modifications to the original Forsberg/Massih model in FRAPCON-3 comprise alterations of gas diffusion constants and a modified treatment of gas re-solution from intergranular bubbles into the fuel matrix, Lanning *et al.* (1997b).

2.4.2.3 Nitrogen release model

The nitrogen present in the fuel stems from fabrication, and its release under subsequent operation occurs as a result of a thermally activated diffusion mechanism. In FRAPCON-3, the release of nitrogen is calculated by the model proposed by Booth (1957).

2.5 Clad waterside corrosion

The models related to clad waterside corrosion have been changed from FRAPCON-2 to FRAPCON-3, in order to allow corrosion of high burnup fuel rods to be modeled more accurately.

2.5.1 Oxide growth

The clad corrosion models in FRAPCON-3 are taken from the Electric Power Research Institute (EPRI) steady-state fuel analysis code ESCORE, Fiero *et al.* (1987). Distinct models are used for BWR and PWR conditions, and the applicable model is automatically selected for each axial segment, based on the relationship of the local coolant temperature to the saturation temperature. The models are fairly simple, and do not consider the influence of coolant chemistry, clad heat treatment or alloy composition on the corrosion rate.

2.5.1.1 BWR conditions

Under BWR conditions, the oxide layer thickness δ_{ox} is assumed to grow according to

$$\frac{\mathrm{d}\delta_{ox}}{\mathrm{d}t} = C_0 e^{-Q_0/RT_{co}} + \frac{C_1 q'}{r_{co}} \tag{2.26}$$

where r_{co} and T_{co} are the clad outer radius and temperature, and q' is the linear heat generation rate. C_0, C_1 and Q_0 are constant model parameters and R is the universal gas constant.

2.5.1.2 PWR conditions

Under PWR conditions, growth of the oxide layer is calculated trough

$$\frac{\mathrm{d}\delta_{ox}}{\mathrm{d}t} = \begin{cases} \dfrac{C_2}{\delta_{ox}^2} e^{-Q_1/RT_{co}} & \delta_{ox} < 2\mu\mathrm{m} \\ \left(C_3 + C_4 \phi^{0.24}\right) e^{-Q_2/RT_{co}} & \delta_{ox} \geq 2\mu\mathrm{m} \end{cases} . \qquad (2.27)$$

Here, ϕ is the fast neutron flux (>1 MeV), whereas C_2, C_3, C_4, Q_1 and Q_2 are constant model parameters.

Comment:

It is clearly stated in the documentation to FRAPCON-3 that the oxide growth models are identical to those in ESCORE. However, we have actually found two differences:

1) The transition in PWR oxide growth does not occur at a fixed oxide thickness of 2 μm in ESCORE, but at a thickness that is dependent on temperature. At T_{co}=600 K, the transition is assumed to take place at an oxide thickness of 2.22 μm.
2) The thermal conductivity of the oxide layer is assumed to be constant (1.68 W/mK) in ESCORE, whereas it is correlated to the clad temperature in FRAPCON-3. As can be seen from figure 2.10, the oxide thermal conductivity used in FRAPCON-3 is about 2.0 W/mK at normal operating temperatures of the clad material.

The latter difference between FRAPCON-3 and ESCORE is important, since FRAPCON-3 will predict lower clad outer temperatures and thereby also lower growth rates for the clad oxide than the original ESCORE model. To this end, it should be noticed that the ESCORE model is known to predict slow oxidation, in comparison with other corrosion models. Figure 2.11 shows a comparison of various PWR oxidation models, reported by Limbäck (1996). With reference to figure 2.11 and the comments made above, it is thus likely that FRAPCON-3 underpredicts the oxide growth rate.

2.5.2 Clad hydrogen pickup

The increase in clad hydrogen content due to the zirconium-water reactions is in FRAPCON-3 assumed to be proportional to the oxide layer thickness. The proportionality constant corresponds to a hydrogen pickup fraction[1] of 0.12 and 0.15 under BWR and PWR conditions, respectively.

2.5.3 Crud growth

The crud layer growth is in FRAPCON-3 modeled by the relation

$$\delta_{crud}(t) = C^0_{crud} + C^1_{crud}\, t\,, \qquad (2.28)$$

where t is the time and C^0_{crud}, C^1_{crud} are user-supplied constants. The crud layer thickness and growth rate are thus assumed to be uniform along the fuel rod.

[1] Pick-up fraction: The fraction of the total amount of hydrogen, created by zirconium-water reactions, that enters into the clad material.

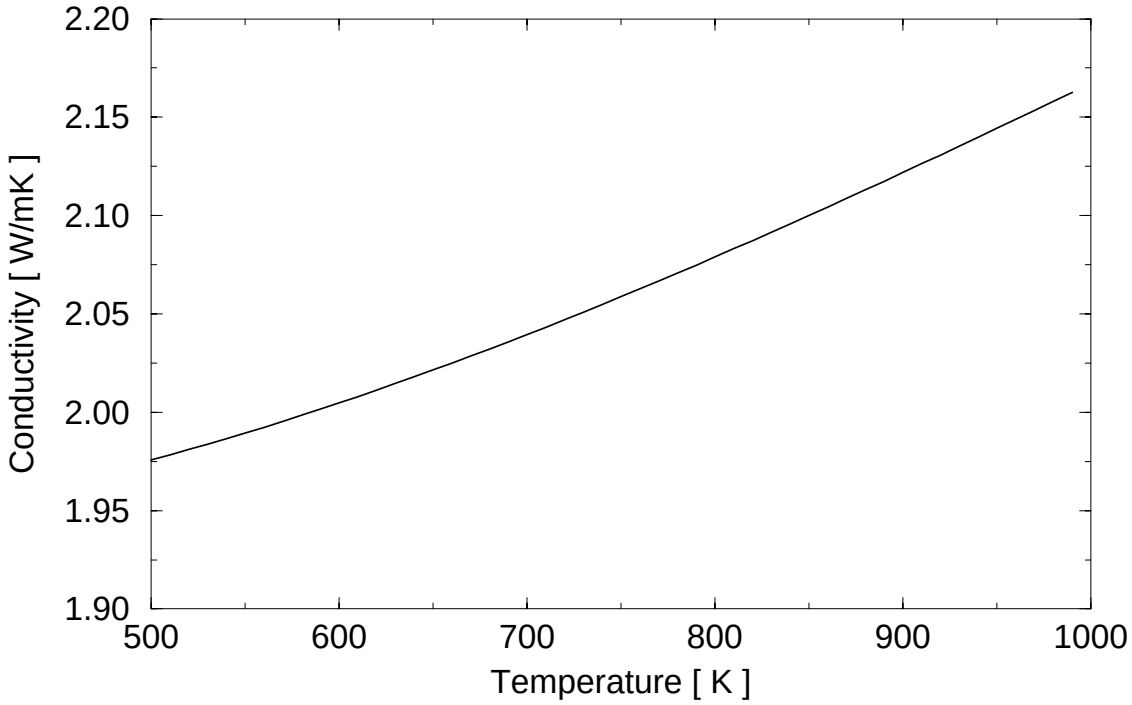

Figure 2.10: Thermal conductivity of ZrO_2 as a function of temperature, as modeled in FRAPCON-3.

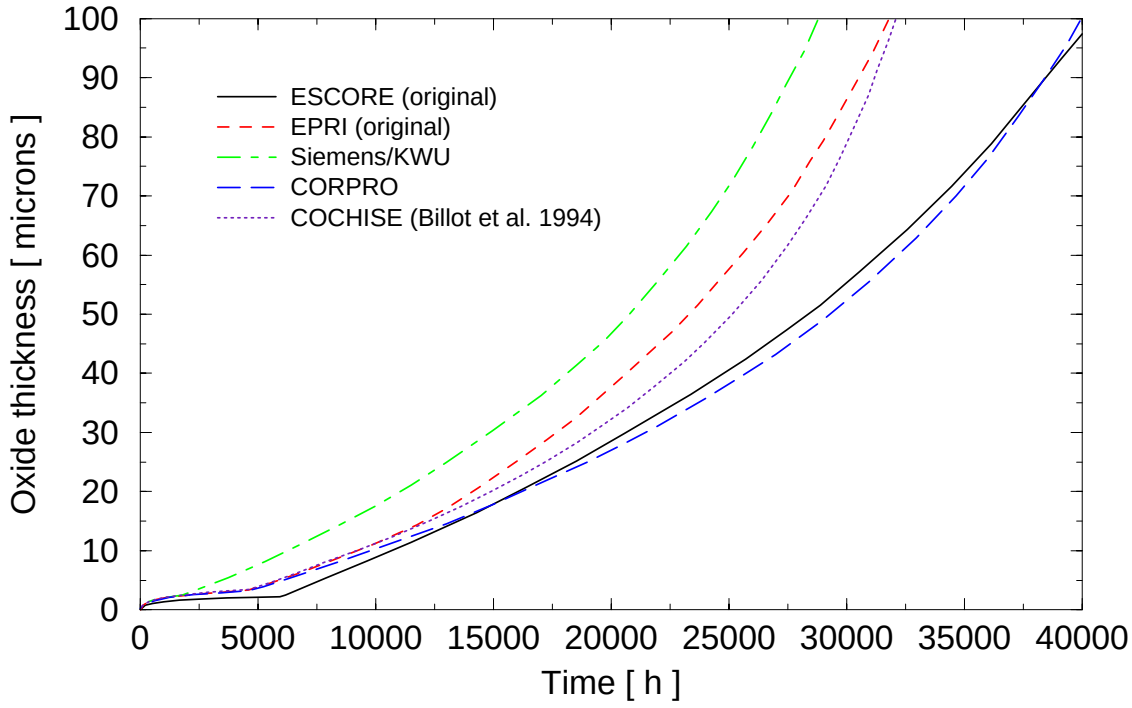

Figure 2.11: Comparison of oxide growth models for PWR conditions. From Limbäck (1996).

3 FRAPCON-3 interface

3.1 Input

All input data needed by FRAPCON-3 are entered via a single text file. The input data basically comprise

- Fuel rod dimensions and design information
- Applied power history and axial power shapes
- Coolant inlet conditions with respect to time
- Discretization and modeling options

The use of a single input file is convenient when cases with simple power histories and constant coolant conditions are analyzed. However, for analyses of cases with complex time-dependent input, a system allowing import of time-dependent input from several files would be preferable.

Keywords are used for entering various parameters in the input file, and by setting a switch to the desired system of units, parameter values can be given in either SI- or British units. The input file is divided into three blocks

- Case control and problem size parameters
- Fuel design and operation data
- Evaluation model options

The first input block contains data on the model size and radial/axial discretization to be used in the analysis. In FRAPCON-3, there are several limitations on the allowable problem size, as shown in table 3.1.

Parameter	***Allowable range***
Time steps	1 - 400
Axial segments	1 - 18
Axial power profiles	1 - 20
Radial nodes in fuel thermal analysis	1 - 25
Radial nodes in fuel FGR analysis	6 - 50

Table 3.1 Limitations on model size parameters in FRAPCON-3.

3.2 Output

Output from FRAPCON-3 is provided to the user in the form of tabulated data and in the form of graphical plots (optional). The capability also exists to supply the calculational results for steady-state initialization of the FRAPTRAN computer code, Cunningham *et al.* (2001).

3.2.1 Tabulated data

FRAPCON-3 provides tabulated output data on the calculated fuel rod thermal-, mechanical, and gas response in the following forms

- Axial segment data
- Power-time step data
- Summary data

All tabulated data are written to a single text file, time step by time step, and the file can reach considerable size (tens of megabytes) in analyses with many time steps or fuel rod axial segments. In contrast to the input procedures, there is no switch for obtaining output in either SI-or British units, and most output is printed in both systems.

The axial segment data present local information on power, time stepping, and burnup. Also presented are rod radial temperature distribution, coolant temperature, clad stresses and strains (both recoverable and permanent), gap conductance, fuel-clad contact pressure, and clad-to-coolant heat transfer information.

The power-time step data present rod burnup, void volumes and associated temperatures, mole fractions of constituent gases and release fractions, total moles of rod gas, and rod gas pressure. Also, this printout of data presents stresses, strains, temperatures, and stored energy as a function of axial position.

The summary data present time-dependent information about the hot axial region. This includes temperatures of the fuel, clad and fuel-clad gap. Information is also given on fuel-clad contact pressure, clad stresses and strains, fuel outside diameter, gap conductance, gas pressure, clad oxide thickness and hydrogen uptake.

3.2.2 Graphical output

The most important fuel rod parameters can be plotted graphically with respect to time or burnup with the aid of a general graphics program, `xmgr`, (Turner, 1991). This program is thus not a part of FRAPCON-3, and the procedures for how `xmgr` is linked to the code are not documented.

3.3 Interface to FRAPTRAN

FRAPCON-3 has the capability to export calculated results to the transient fuel analysis code FRAPTRAN via an interface file. The information provided to FRAPTRAN consists of permanent burnup effects, such as clad creep, fuel swelling, fuel densification, normalized radial power and burnup profiles, and fission gas inventory.

The interface file used by FRAPTRAN can also be used for steady-state initialization of other codes for fuel rod transient analyses. As an example, an interface between FRAPCON-3 and the SCANAIR code has recently been developed, Jernkvist (2002).

4 Code implementation and documentation

4.1 History

The FRAPCON computer code and its supporting material properties package MATPRO date back to the mid-seventies. The very first version, FRAPCON-1, was largely based on the FRAP-S3 code developed at INEEL, but in FRAPCON-1, the FRAP-S3 code was enhanced by introducing an efficient subcode for thermal analysis, developed at PNNL.

The next version, FRAPCON-2, involved improvements that added much complexity to the code. The major improvements in FRAPCON-2 with respect to FRAPCON-l include three advanced options for mechanical analysis, four additional fission gas release options, and an uncertainty analysis option.

In FRAPCON-3, a major step toward code simplification has been taken by removing rarely used options and models. The simplifications include removing all but one of the mechanical models, removing all but the ANS 5.4 fission gas release model, removing the automated uncertainty model and simplifying both the code input and output. The code has also been enhanced by

1) Incorporating a finite difference heat conduction model, which is required for improved spatial definition of heat generation and conduction; see section 2.2.1
2) Adding the transient two-stage fission gas release model by Forsberg and Massih; see section 2.4.2.2
3) Adding new radial power/burnup distribution models and fuel thermal conduction models, to allow the code to model high burnup fuel rods
4) Incorporating the UNIX-based graphics program `xmgr`; see section 3.2.2

Albeit the simplifications gained by removing obsolete or rarely used models in FRAPCON-3, the source code is still complex. This is in part due to the programming language, Fortran-IV, which offers very limited possibilities to code modularization and transparent data transfer in comparison with modern languages.

4.2 Code structure

The computational flow in FRAPCON-3 is depicted in figure 4.1. The calculation begins by processing input data. Next, the initial fuel rod state is determined through a self-initialization calculation. Time is advanced according to the input-specified time-step size, a steady-state solution is performed and the new fuel rod state is determined. The new fuel rod state provides the initial state conditions for the next time step. The calculations are cycled in this manner for a user-specified number of time steps, and the solution for each time step consists of

1) Calculating the temperature of the coolant, fuel and clad
2) Calculating fuel and clad deformation
3) Calculating the heat conductance across the pellet-to-clad gap
4) Calculating the fission gas release, fuel rod void volume and internal gas pressure

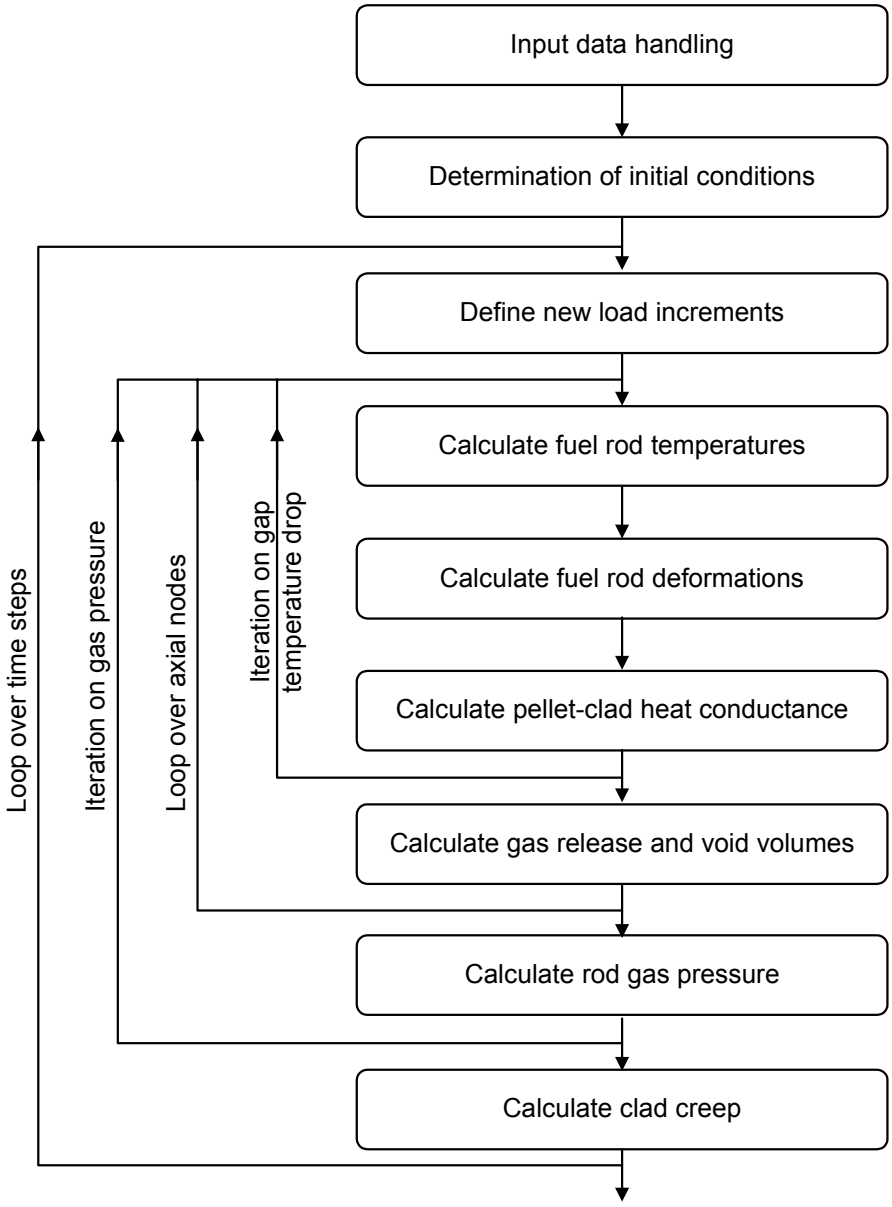

Figure 4.1 Flowchart of FRAPCON-3.

Each of these calculations is made via separate high-level subroutines, represented by boxes in figure 4.1. As shown in the figure, the fuel rod response for each time step is determined by repeated cycling through two nested loops of iterative calculations, until the fuel-cladding gap temperature difference and rod internal gas pressure converge.

The fuel rod temperature distribution and deformation are alternately calculated in the innermost loop. On the first cycle through this loop for each time step, the pellet-to-clad heat conductance is taken from the previous time step. Then the new fuel rod temperature distribution is computed. This temperature distribution feeds the deformation calculation by influencing the fuel and cladding thermal expansions and the cladding stress-strain relation. An updated fuel-cladding gap size is calculated and used in the gap conductance calculation on the next cycle through the inner loop. This cyclic process through the inner loop is repeated until two successive cycles calculate essentially the same temperature drop across the pellet-to-clad gap.

The outer loop of calculations is cycled in a manner similar to that of the inner loop, but with the rod gas pressure being determined during each iteration. The calculation alternates between the fuel rod void volume-gas pressure calculation and the fuel rod temperature-deformation calculation. On the first cycle through the outer loop for each time step, the gas pressure from the previous time step is used. For each cycle through the outer loop, the number of gas moles is calculated and the updated gas pressure computed and fed back to the deformation and temperature calculations (the inner loop). The calculations are cycled until two successive cycles calculate essentially the same gas pressure, then a new time step is begun.

Comment:
The criterion for convergence in the thermo-mechanical analysis (the innermost loop in figure 4.1) is somewhat dubious. In most fuel performance analysis codes, the convergence criteria are focused on the fuel centerline temperatures. The choice of the gap temperature drop as an iteration parameter in FRAPCON-3 is not clear.

As shown in figure 4.1, the clad creep is calculated *outside* the iterative loops, which implies that creep is assumed to have only a limited effect on the fuel rod thermo-mechanical response under each time step. This assumption actually puts a restriction on the allowable time step length, in particular at end-of-life fuel rod conditions, when the pellet-clad gap is closed and the clad creep rate can be significantly enhanced by stresses from pellet-clad mechanical interaction.

4.3 Programming language and style

The FRAPCON-3 code and the MATPRO material properties package are written in Fortran-IV, which is a predecessor to the Fortran-66 language. It should be noticed that Fortran-IV is a programming language developed by IBM for use on early IBM mainframe machines, and does not fully conform to the standardized Fortran-66 language. Moreover, the Fortran-66 standard has been succeeded by both Fortran-77 and Fortran-90, with Fortran-95 underway.

Today's compilers for Fortran-77 and Fortran-90 can usually be made to accept source code written also in Fortran-IV, but there is a risk that FRAPCON-3 in its present source form cannot be compiled on compilers for Fortran-95. Several obsolete language elements in Fortran-IV are excluded from the Fortran-95 standard, and are therefore unlikely to be supported by future compilers. As an example, the source code to FRAPCON-3 is studded with Hollerith character string edit commands, which are not supported in Fortran-95.

It should be noticed, that FRAPCON-3 can be used on both UNIX workstations and personal computers with the Microsoft Windows operating system. A prerequisite for use under Microsoft Windows is that the Digital/Compaq Visual Fortran Compiler, version 5 or 6, is installed on the target machine.

The total number of subroutines in FRAPCON-3 is over 200, but many of these routines belong to the MATPRO material properties package. The source code is difficult to read, modify and extend. This is partly due to lack of comments in the source code and supporting documentation on the code structure, but it is also a result of the programming language itself. Much could be gained by rewriting the top-level subroutines of the code in Fortran-90, which has much better support for code modularization and transparent data transfer than Fortran-IV.

Another difficulty with the code is the mixed use of SI- and British units; transformations between the two systems are frequent, and it is not always clear where and when a certain system is used. This is unfortunately not only true for the source code, but also for the code documentation.

4.4 Code documentation

There are two documents describing FRAPCON-3 and its application

- A general code description, which briefly presents models, computational methods and code structure, Berna *et al.* (1997)
- An integral assessment report, which presents the performed verification and calibration of the code, Lanning *et al.* (1997a)

In addition, there are two documents related to the MATPRO material properties package, which is extensively used in FRAPCON-3

- The original MATPRO package, Hagrman *et al.* (1981)
- The models in MATPRO, which have been extended or re-calibrated for high burnup fuel rod applications, Lanning *et al*. (1997b)

The documents listed above give a good overview of the code, its modeling bases and validation. However, many details in the documents do not correspond to the actual content of the source code; over the years, the code has probably been modified without introducing appropriate changes to the documents. Moreover, certain information is scarce in the above documents. Firstly, a user's manual to FRAPCON-3 would be desirable, in which guidelines on installing and running the program are given together with a thorough description of input and output. Secondly, a maintenance manual or programmer's manual is desirable for those who intend to modify or extend the code. There is a significant gap between the general code description and the Fortran source code, which should be bridged by such a manual.

5 Code calibration and verification

Models applied in FRAPCON-3 for various physical phenomena are usually verified and validated through data from separate effect tests and well-controlled laboratory experiments. This is for instance the case for all the material properties correlations used in FRAPCON-3.

The verification of individual models has been complemented with an integral assessment of the entire code. The integral assessment was done by comparing the code predictions for fuel temperatures, fission gas release, rod internal void volume, fuel swelling, clad creep and axial growth, clad corrosion and hydriding to data from in-reactor irradiation experiments and post-irradiation examination programs.

In the case of fuel temperatures and fission gas release, experimental data are scarce for high burnup fuel, and the data sets were actually also used to calibrate the thermal models and the fission gas release model. Therefore, the code predictions have also been compared to additional "independent" data sets for fuel temperatures and high-burnup fission gas release. The extent of the integral assessment is described in the following subsections, and key results are presented.

5.1 Assessment data base

The in-reactor experiments used for code assessment were selected on the criteria of providing well characterized fuel rod design data and operational histories, and spanning the ranges of interest for both design and operating parameters. Thus, the fuel rods represent both boiling water reactor (BWR) and pressurized water reactor (PWR) fuel types, with pellet-to-clad gap sizes within, above, and below the normal range for power reactor rods. The fill gas is usually pure helium, but some cases are included with xenon and helium-xenon fill gas mixtures.

In the selected cases, the rod linear heat generation rates range up to 58 kW/m, and the rod-average fuel burnups range up to 74 MWd /kgU. The end-of life (EOL) fission gas release ranges from less than 1% to greater than 30% of the produced quantity.

In all, data from 45 fuel rods were used in the integral assessment of FRAPCON-3, Lanning *et al.* (1997a). Thirty of these cases were used for calibration of thermal and fission gas release models, and thus constitute the primary experimental database for FRAPCON-3. The remaining fifteen cases were not used for calibration, and thus provided independent verification of the code predictability. These cases were preferably taken from experimental programs that were independent of the experimental data programs used for code calibration, and where either the fission gas release or fuel temperatures were measured and rod powers were accurately known. These independent test cases will not be further commented here.

All of the thirty fuel rods that were used for calibration of the code provide well-qualified fuel rod power histories and design data, and they have all undergone post-irradiation examinations. The selected cases include 20 fuel rods with steady-state power operation and 10 fuel rods with steady-state irradiations, followed by an end-of-life power ramp. The fuel rods in the latter group were only used for calibration of the fission gas release model, whereas data from the first group were used for calibration of other models as well.

Reactor (Type)	Assembly Rod(s)	Rod average BU [MWd/kgU]	Max LHGR, rod average [kW/m]	FGR fraction at end-of-life [-]	Temp at BOL	Temp vs BU	FGR at EOL	Rod void volume	Rod axial growth	Clad Creep	Clad oxide
Halden	HUHB										
	18	80	37.9	< 0.01		x					
Halden	IFA432										
BWR	1	30	38.9	0.20	x						
	2	30	41.1	0.30	x						
	3	40	41.1	0.10	x	x					
Halden	IFA513										
BWR	1	12	40	< 0.01	x						
	6	12	40	0.02	x						
Halden	IFA429										
PWR	DH	74	41.5	0.24			x				
BR-3	W-house										
PWR	36-I-8	61.5	41.3	0.34			x	x			
	111-I-5	48.6	45.7	0.14			x	x			
	24-I-6	60.1	43.7	0.22			x	x			
	28-I-6	53.3	34.4	0.13			x				
BR-3	BNFL										
PWR	DE	41.5	46.8	0.11			x				
NRX											
PWR	LFF	2.2	58.4	0.17			x				
NRX											
PWR	CBP	2.6	55.1	0.14			x				
EL-4	4110										
PWR	AE2	6.2	57.7	0.22			x				
	BE2	6.6	58.4	0.16			x				
ANO-2	D040										
PWR	TSQ002	53	22.8	< 0.01			x	x	x	X	x
Oconee	1D45										
PWR	15309	50	25.9	< 0.01			x	x	x	X	x
Monticello	MTAB099										
BWR	A1	45	22.7	0.30			x		x	X	x
TVO-1	HBEP										
BWR	H8/36-6	51.4	23.4	0.11			x		x		x

Table 5.1 Steady-state test data used for integral assessment of FRAPCON-3. Crosses indicate which test cases were used for assessing particular parameters.

Test reactors:

Halden: Halden, Norway
BR-3: Mol, Belgium
NRX: Chalk River, Ontario, Canada
EL-4: Monts D'Arree, France

Commercial reactors:

ANO-2: Arkansas Nuclear One, unit 2, Arkansas, U.S.A.
Oconee: Oconee, South Carolina, U.S.A.
Monticello: Monticello, Minnesota, U.S.A.
TVO-1: Teolisuuden Voima OY, unit 1, Finland

The steady-state and power-ramp cases are summarized in tables 5.1 and 5.2. Table 5.1 also indicates which test cases were used for assessing a certain parameter. It is noteworthy that the cases used to assess clad oxidation and deformation are limited to the full-length power reactor rods, because only those rods operated in prototypic neutronic and coolant conditions, both of which affect creep, axial growth, and metal-water reactions.

Reactor (Type)	Assembly Rod(s)	Rod average BU [MWd/kgU]	Max LHGR, rod average pre-ramp [kW/m]	Max LHGR, rod average under ramp [kW/m]	FGR fraction, pre-ramp [-]	FGR fraction, post-ramp [-]	Ramp hold time [h]
Obrigheim/							
Petten	D200	25	27.1	45.3	0.07	0.38	48
PWR	D226	44	27.3	43.0	0.04	0.44	48
Obrigheim/							
Studsvik	PK6-2	35	26.9	40.0	-	0.04	12
Superramp	PK6-3	35	26.9	43.0	-	0.07	12
PWR	PK6-S	35	26.9	41.0	-	0.06	12
Studsvik							
Interramp	16	21	43.0	47.9	-	0.16	24
BWR	18	18	36.0	41.0	-	0.04	24
Halden/	IFA148						
DR-2	F7-3	35	43.7	42.6	0.06	0.12	24
BWR	F14-6	27	34.2	44.1	0.06	0.22	24
	F9-3	33	43.7	43.7	0.07	0.18	44

Table 5.2 End-of-life transient test data used in integral assessment of FRAPCON-3. These cases were used for assessment of the Forsberg/Massih transient fission gas release model only.

Test reactors:

Petten: Petten, The Netherlands
Studsvik: Nyköping, Sweden
Halden: Halden, Norway
DR-2: Risø, Denmark

Commercial reactors:

Obrigheim: Obrigheim, Baden-Würtemberg, Germany

Comment:

As evidenced by tables 5.1 and 5.2, the data base used for code calibration comprises 12 BWR and 17 PWR fuel rods. However, in the complementary data based used for independent verification, there were 11 BWR and 4 PWR rods. In total, the data base thus comprises about the same number of BWR and PWR rods.

It should be noted, that the test data base contains no (U,Pu) or (U,Gd) mixed oxide fuel rods whatsoever. Further assessment of the code is therefore necessary, before it can be applied to (U,Pu) mixed oxide or burnable absorber fuel.

5.2 Fuel temperature

Predicted and measured fuel center temperatures from instrumented Halden reactor test assemblies have been used to evaluate the code's ability to predict beginning-of-life (BOL) temperatures and through-life temperature histories. The BOL temperature comparisons were used for calibration of the fuel relocation model presented in section 2.3.1. The relocation model was thereby tuned to give best possible agreement between measured and predicted fuel center temperatures.

The BOL temperature database includes not only rods filled with helium, but also rods with xenon and xenon-helium filled gaps and rods with pellet/clad gap sizes both larger and smaller than normal. These variations provide the bases for code evaluation beyond the normal ranges for gap size and thermal resistance.

A comparison between measured and predicted BOL centerline temperatures is shown in figure 5.1. The code predictions are typically within 50 K of measured values; somewhat larger deviations are found for the xenon-helium filled rod IFA513-R6.

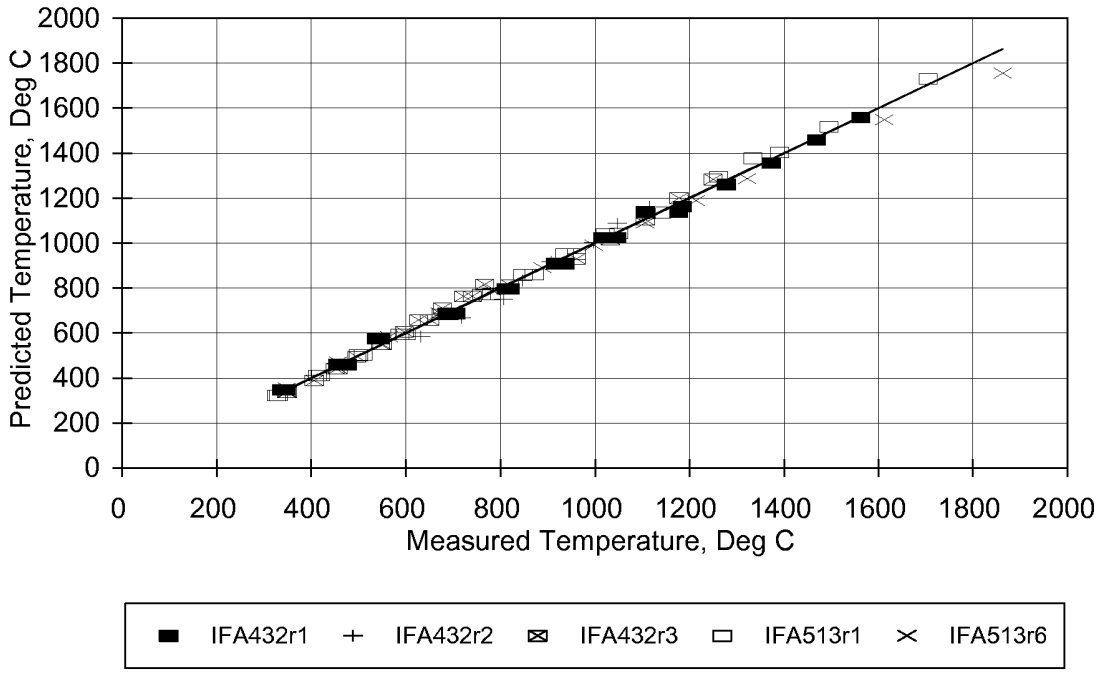

Figure 5.1: FRAPCON-3 predictions vs measured BOL fuel center temperatures. From Lanning et al. (1997a).

The comparisons of measured and predicted through-life fuel center temperature histories were done with two goals in mind: The first goal was to check on the trend of thermal conductivity degradation with burnup, and the second goal was to check on the effect of thermal feedback caused by fission gas release and consequent contamination of the initial helium fill gas with lower-conductivity fission gas.

The effect of thermal conductivity degradation was studied by comparing code predictions with experimental data from two fuel rods, in which the confounding effects of thermal feedback are weak. The first rod, HUHB-R18, had relatively low operating temperature, whereas the second rod, IFA432-R3, had a small pellet-to-clad gap size.

The differences between predicted and measured fuel centerline temperatures for these two rods are shown with respect to rod average burnup in figure 5.2. The predicted temperatures near BOL exceed the measured values, approach equality with the measurements over a burnup range from 15 to 35 MWd/kgU, and are less than the measured values from about 40 MWd/kgU to the limit of the reported data.

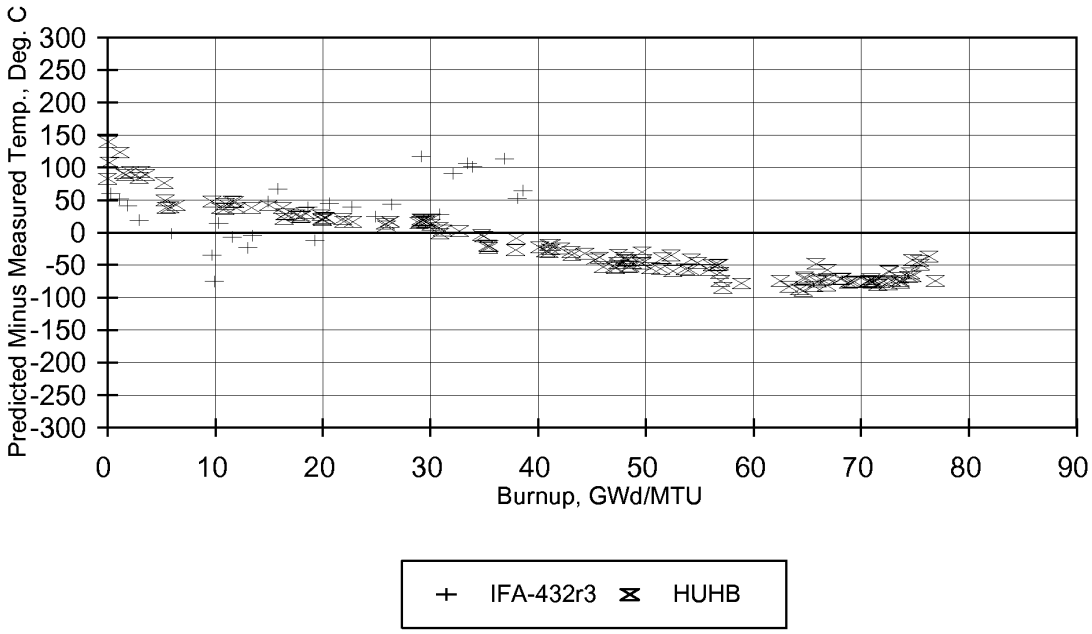

Figure 5.2: Differences between predicted and measured fuel centerline temperatures, plotted with respect to rod average burnup. From Lanning et al. (1997a).

Comment:
Figure 5.2 reveals a bias in the temperature predictions, and it is obvious that the fuel centerline temperatures in the Halden HUHB rod are consistently underpredicted at 40 MWd/kgU and above. In this range of burnup, the pellet-clad gap is usually closed, and uncertainties in the gap heat transfer model do not significantly affect the fuel temperature predictions. A likely explanation to the bias is therefore that the degradation of fuel thermal conductivity with burnup is underestimated by the FRAPCON-3 model, as discussed in section 2.2.1. Definite conclusions cannot be drawn solely from figure 5.2, in which results from a single fuel rod are presented, but the assumption is also supported by the comparison with results obtained from fuel centerline temperature measurements on numerous rods in the Halden experimental reactor, as presented in figure 2.5.

5.3 Fission gas release

The code's ability to predict fission gas release has been assessed based on comparisons to data from 24 fuel rods. This data base comprises 14 rods with power histories that are relatively steady-state through the irradiation life, and 10 rods with an increase in rod power at EOL, to simulate an overpower transient or operational occurrence.

The results presented here are due to the two-stage fission gas release model by Forsberg and Massih. As described in section 2.4.2.2, this model is intended for fission gas release under mild transients, such as the EOL power ramps studied here.

Also the ANS-5.4 fission gas release model has been assessed, and the results show that the model provides a good prediction of fission gas release for the fuel rods with steady-state power histories, but on average underpredicts fission gas release for the fuel rods with power ramps for a few hours duration. This is not too surprising, since this model is not at all intended to predict power transients.

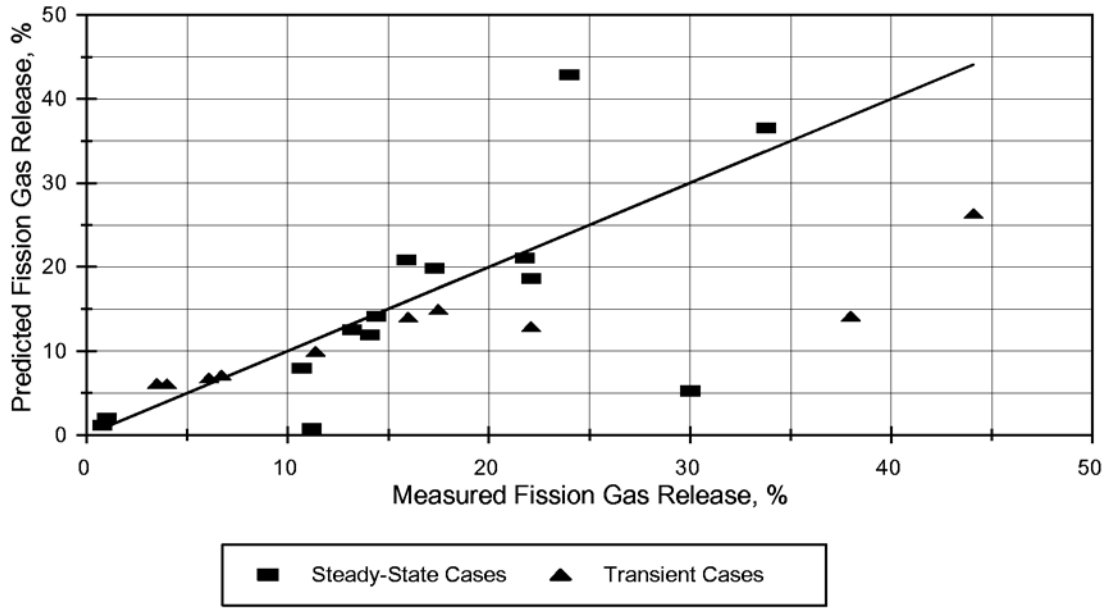

Figure 5.3: FRAPCON-3 predictions vs measured fission gas release. The predictions are made by use of the Forsberg/Massih model. From Lanning et al. (1997a).

The predicted fission gas release from the Forsberg/Massih model is compared with the measured values in figure 5.3. The agreement is fairly good; the outliers in the data are related either to commercial reactor fuel rods, whose local rod power histories have large uncertainties, or to rods with unstable (large densification) fuel pellets.

Comment:

The Forsberg/Massih fission gas release model in FRAPCON-3 corresponds to the original work by Forsberg and Massih (1985) with slight modifications, as described in section 2.4.2.2. The model in the original model has recently been improved by the authors, Hermansson and Massih (2002), and as a result of these improvements, the accuracy of the applied numerical method has been significantly enhanced in the low release regime, *i.e.* for release fractions less than 5%. For higher release fractions, the original method proposed by Forsberg and Massih is known to be very accurate, (Lassman and Benk, 2000).

It should also be mentioned that the effect of UO_2 grain growth on fission gas release is not taken into account in the original model by Forsberg and Massih, but in recent years, the model has been extended to include the effect of grain boundary sweeping, (Forsberg and Massih, 2001). However, this extended model is not yet included in FRAPCON-3.

5.4 Rod internal void volume

Five fuel rods have been used to assess the capability of FRAPCON-3 to accurately calculate fuel rod void volumes for high burnup. The selected cases include two full-length rods (Rod TSQ002 from ANO-2 and Rod 15309 from Oconee) and three short (112 cm long) rods (36-I-8, 111-I-5, and 24-I-6) that were irradiated in the BR-3 reactor. The set includes only PWR fuel rods with standard Zircaloy-4 clad materials. The average burnup levels achieved on these rods range from 48.6 to 61.5 MWd/kgU.

Table 5.3 presents the measured and calculated void volumes at end-of-life for the five fuel rods. The calculations were made at 25 ºC, which should be reasonably close to the temperature at which the data were collected. A range of values for void volume is provided for Oconee rod 15309; this is the range of void volumes measured from 16 sibling fuel rods from the same assembly.

Table 5.3 shows that the predicted void volumes of the considered rods are within 10% of the measured values.

Reactor	Rod	Rod average burnup [MWd/kgU]	Measured void volume [cm^3]	Calculated void volume [cm^3]	Relative error [%]
BR-3	36-I-8	61.5	8.32	8.77	5.3
BR-3	111-I-5	48.6	8.46	9.39	11.0
BR-3	24-I-6	60.2	8.05	8.83	9.8
ANO-2	TSQ002	53	17.8	18.3	2.7
Oconee	15309	49.5 to 49.9	26.2 to 28.2	25.1	-11.0 to -4.4

Table 5.3: Measured end-of-life void volumes in comparison with FRAPCON-3 predictions for five high burnup PWR fuel rods.

Comment:
The evolution with time of fuel rod internal void volume is affected primarily by the fuel swelling and the clad creep. To this end, it should be noticed that the model for fuel swelling in FRAPCON-3 has been calibrated to a comparatively large number of measurements on high burnup fuel, and the current model thus differ from the original MATPRO model applied in earlier versions of FRAPCON, Lanning *et al.* (1997b).

5.5 Clad corrosion

In contrast to earlier versions of FRAPCON, the predictions of cladding waterside corrosion are in FRAPCON-3 based on the uniform oxidation models developed for the ESCORE computer program, Fiero *et al.* (1987). The correct implementation of these models in FRAPCON-3 has been verified by comparing the code predictions with those obtained by the original, stand-alone versions of the models.

However, as mentioned in section 2.5.1, there is a significant difference between FRAPCON-3 and ESCORE with respect to the model for oxide thermal conductivity. The effects of this difference have not been studied in the performed assessment.

Four fuel rods from table 5.1 were selected to demonstrate the capability of FRAPCON-3 to accurately calculate fuel rod waterside oxidation and hydrogen pick-up at high burnup. The cases selected include four full-length rods (rod TSQ002 from ANO-2, rod 15309 from Oconee, rod A1 from Monticello, and rod H8/36-6 from TVO-1). The set includes both PWR and BWR fuel rods that are either standard Zircaloy-4 in PWR's or Zircaloy-2 in BWR's. The comparison shows that the predictions of waterside oxidation and hydrogen pick-up are in fair agreement with the considered experimental data.

5.6 Clad deformation

As described in section 2.3.2, the model for clad creep in FRAPCON-3 is derived from BWR data, and not suited for accurate predictions of creep deformation in stress relief annealed (SRA) clad materials used in PWR's. The creep model in FRAPCON-3 was used also in earlier versions of the code.

The model for irradiation induced clad axial growth is new to FRAPCON-3, and based on the work of Franklin (1982). This model provides best-estimate predictions of axial growth data in PWR's, but is in FRAPCON-3 also applied to BWR conditions, simply by reducing the PWR growth rate by 50%, Lanning *et al.* (1997b).

Table 5.4 shows a comparison of predicted and measured axial growth in four rods from the database used for integral assessment of FRAPCON-3. As shown in the table, the predictions for the two PWR rods are better than those obtained for the BWR rods. However, the axial growth is underpredicted for all rods.

Reactor (Type)	Rod	Rod average burnup [MWd/kgU]	Measured rod growth [%]	Calculated rod growth [%]	Relative error [%]
ANO-2					
PWR	TSQ002	53.0	0.83 to 1.11	0.85 to 0.96	-7.0
Oconee					
PWR	15309	50.0	0.79 to 0.91	0.79	-7.0
Montecillo					
BWR	A1	45.0	0.52	0.39	-25.0
TVO-1					
BWR	H8/36-6	51.4	0.30	0.25	-17.0

Table 5.4: Measured clad axial growth in comparison with FRAPCON-3 predictions for four high burnup fuel rods.

Comment:

The model applied for irradiation-induced clad growth in FRAPCON-3 is merely an empirical correlation, derived from axial growth measurements on PWR fuel rods. Since irradiation induced growth is strongly dependent on the material texture and heat treatment, a better approach would be to introduce a mechanistic model, in which these effects are considered, Kubo (1990).

6 Concluding remarks

In this report, we have evaluated the FRAPCON-3 computer code with respect to its range of application, modeling capability, user friendliness and supporting experimental data base. We conclude that FRAPCON-3 is applicable to thermo-mechanical analyses of both BWR and PWR fuel rods under steady-state operational conditions, and to some extent also to slow power excursions. With the introduction of a new set of models for high burnup phenomena, FRAPCON-3 lends itself to analyses of fuel rods ranging up to 65 MWd/kgU in rod average burnup. Limitations in the applicability primarily concern $(U,Pu)O_2$ and $(U,Gd)O_2$ fuel and analyses of pellet-clad mechanical interaction.

The models and numerical methods in FRAPCON-3 are deliberately simple, in order to make the code transparent and easy to modify and extend. In fact, FRAPCON-3 has been slimmed and simplified with respect to earlier versions of the code. Accordingly, the fundamental equations for heat transfer and structural analysis are solved in one-dimensional (radial) and stationary (time-independent) form. If a transient phenomenon is to be studied, FRAPCON-3 can be used to calculate the burnup dependent pre-transient fuel rod conditions, and the actual transient then modeled with FRAPTRAN, which is a sibling code, comprising time-dependent formulations of the same fundamental equations as solved in FRAPCON-3.

The simplicity of FRAPCON-3 results in short execution times, typically about 10 seconds, which makes the code feasible for probabilistic analyses. The code is also fairly straightforward to use; fuel rod design data and time histories of fuel rod power and coolant inlet conditions are input via a single text file, and the corresponding calculated variation with time of important fuel rod parameters are printed to a single output file in textual form. The results can also be presented in graphical form through an interface to the general graphics program `xmgr`.

Unfortunately, a comprehensive user's manual to the code is lacking, but models and their experimental support are on the other hand well documented. This is particularly true for the materials property package MATPRO, which is extensively used in the code.

Both FRAPCON-3 and the MATPRO package are largely written in Fortran-IV, which is an archaic, non-standard dialect of the Fortran programming language that has been succeeded by Fortran-66, -77, -90 and -95. For this reason, there is a risk that FRAPCON-3 in its present source form cannot be compiled on modern compilers for Fortran-95.

The FRAPCON-3 code has been subjected to an integral assessment with respect to its capability to predict fuel temperatures, fission gas release, rod internal volume, clad oxidation, creep and axial growth in high burnup fuel rods. Experimental data from 45 fuel rods, of which 21 were PWR and 23 BWR, were used in the assessment. Thirty of these rods were used for calibration of thermal- and fission gas release models, whereas the remaining fifteen rods were not used for calibration, and thus provided independent verification of the code predictability. The assessment confirms the applicability of FRAPCON-3 to high burnup fuel rods, but also reveals weaknesses in particular models. Moreover, it should once again be stressed that the code in its present form is neither intended to, nor verified for, modeling of $(U,Pu)O_2$ and $(U,Gd)O_2$ fuel or detailed analyses of pellet-clad mechanical interaction.

Based on our evaluation, we suggest that the following improvements are made to certain models in FRAPCON-3 that have been found to be less adequate:

1) The improved parameters in the Forsberg/Massih fission gas release model, as proposed by Hermansson and Massih (2002), should be introduced in order to enhance accuracy for low fission gas release fractions.

2) A clad creep model, applicable to PWR operating conditions and clad materials, should be introduced. A conceivable model is the one proposed by Limbäck and Andersson (1996).

3) The model for irradiation induced clad axial growth needs improvements, especially for recrystallization annealed clad materials that are predominantly used in BWR's.

4) Modeling of $(U,Gd)O_2$ fuel rods necessitates introduction of modified models for the fuel power- and burnup distributions, fuel thermal conductivity and fission gas release. Suitable models that can be used in FRAPCON-3 for the above mentioned phenomena have been presented by Massih *et al.* (1992). A model for the radial power distribution in $(U,Gd)O_2$ fuel, which can alternatively be used, is due to Shann *et al.* (1991).

5) According to our evaluation, the clad corrosion model in FRAPCON-3 is prone to underestimate the oxide growth rate, at least for PWR conditions. The model thus needs further verification and calibration to experimental data. Alternatively, the PWR clad corrosion model proposed by Forsberg *et al.* (1995) can be introduced.

6) FRAPCON-3 needs improvements to the clad plasticity model and experimental verification with respect to clad deformations under pellet-clad mechanical interaction. Several instrumented fuel assemblies in the Halden experimental reactor, equipped with either clad axial extensometers or clad diameter gauges, can be used for this purpose, Turnbull (1995). A relocation model, addressing the mechanical behavior of the cracked fuel, should also be introduced into the code and calibrated with the experimental data.

In conclusion, we believe that the FRAPCON fuel rod analysis program has been significantly enhanced by the introduction of high burnup models in version 3 of the code. The predictability of these new models has also on the whole been confirmed by comparisons with relevant experimental data. Although the programming language and style is somewhat archaic, we believe that FRAPCON-3 constitutes a suitable computer code, not overly complex, into which SKI can add new and improved models that satisfy their requirements.

7 References

American Nuclear Society (ANS),
Method for calculating the fractional release of volatile fission products from oxide fuel, ANS5.4 of the Standards Committee of the American Nuclear Society, ANSI/ANS-5.4-1982.

Berna, G. A., Beyer, C. E., Davis, K. L. and Lanning, D.D., *FRAPCON-3: A computer code for the calculation of steady-state, thermal-mechanical behavior of oxide fuel rods for high burnup*, NUREG/CR-6534, PNNL-11513, Vol. 2, prepared for the U.S. Nuclear Regulatory Commission by Pacific Northwest Laboratory, Richland, Washington, 1997.

Berna, G.A., Bohn, M.P., Rausch, W.N., Williford, R.W. and Lanning, D.D., *FRAPCON-2: A computer code for the calculation of steady-state thermal-mechanical behavior of oxide fuel rods,* NUREG/CR-1845, 1980.

Beyer, C.E., Hann, C.R., Lanning, D.D., Panisko, F.E and Parchen, L.J., *GAPCON-THERMAL-2: A computer program for calculating the thermal behavior of an oxide fuel rod,* BNWL-1898, November 1975.

Bohn, M.P., *FRACAS: A subcode for the analysis of fuel pellet-cladding mechanical interaction,* Report TREE-NUREG-1028, April 1977.

Booth, A.H., *A method of calculating fission gas diffusion from UO_2 fuel and its application to the X-2 loop test,* AECL-496, CRDC-721, 1957.

Cunningham, M.E. and Beyer, C.E., *GT2R2: An updated version of GAPCON-THERMAL-2*, Report NUREG/CR-3907, PNL-5178, Pacific Northwest Laboratory, 1984.

Cunningham, M.E., Beyer, C.E., Medvedev, P.G. and Berna, G.A., *FRAPTRAN: A computer code for the transient analysis of oxide fuel rods*, NUREG/CR-6739, PNNL-13576, Volume 1, prepared for the U.S. Nuclear Regulatory Commission by Pacific Northwest Laboratory, Richland, Washington, 2001.

Fidleris, V., *Summary of experimental results on in-reactor creep and radiation growth of Zirconium alloys*, Atomic Energy Review, Vol. 13, No. 1, pp. 51-80, 1976.

Fiero, I. B., Krammen, M.A. and Freeburn, H.R., *ESCORE - the steady-state core reload evaluator code: General description*, EPRI-NP-5100, Project 2061-6 -13 Final Report. Prepared for Electric Power Research Institute, Palo Alto, California, 1987.

Forsberg, K., Limbäck, M. and Massih, A.R., *A model for uniform Zircaloy clad corrosion in pressurized water reactors*, Nuclear Engineering and Design, Vol. 154, pp. 157-168, 1995.

Forsberg, K. and Massih, A.R., *Diffusion theory of fission gas migration in irradiated nuclear fuel UO_2* , J. Nuclear Materials, Vol. 135, pp. 140-148, 1985.

Forsberg, K. and Massih, A.R., *Theory of fission gas release during grain growth*, Paper C05/1 in Proceedings of the 16th International Conference on Structural Mechanics in Reactor Technology (SMiRT-16), Washington DC, August 12-17, 2001.

Franklin, D. G., *Zircaloy cladding deformation during power reactor irradiation,* In: Proceedings of the Fifth International Symposium on Zirconium in the Nuclear Industry, ASTM-STP-754, pp. 235-267, 1982.

Hagrman, D. L., Reymann, G.A. and Mason, G.E., *A handbook of materials properties for use in the analysis of light water reactor fuel rod behavior*, MATPRO Version 11 (Revision 2), NUREG/CR-0479 (TREE-1280), prepared by EG&G Idaho, Inc., Idaho Falls, Idaho for the U.S. Nuclear Regulatory Commission, Washington, D.C., 1981.

Harding, J.H. and Martin, D.G., *Recommendation for the thermal conductivity of UO_2*, J. Nuclear Materials, 166, pp. 223-226, 1989.

Hermansson P., Massih A.R., *An effective method for calculation of diffusive flow in spherical grains*, Submitted to J. Nuclear Materials, 2002.

Ibrahim, E.F., *In-reactor tubular creep of Zircaloy-2 at 260 to 300 °C,* J. Nuclear Materials, Vol. 46, pp. 169-182, 1973.

Jernkvist, L.O., *An interface between FRAPCON-3 and SCANAIR 3.2*, Quantum Technologies Report TR 02-003, 2002.

Jernkvist, L.O. and Manngård, T., *Application of FRAPCON-3 and SCANAIR 3.2 for fuel rod analysis of RIA in LWR's* , Quantum Technologies Report TR 02-006, 2002.

Kubo, T., *Irradiation growth in zirconium alloys under high fluences,* *Res Mechanica*, Vol. 29, pp. 289-312, 1990.

Lanning, D. D., Beyer, C. E. and Berna, G. A., *FRAPCON-3: Integral assessment*, NUREG/CR-6534, PNNL-11513, Vol. 3, prepared for the U.S. Nuclear Regulatory Commission by Pacific Northwest Laboratory, Richland, Washington, 1997a.

Lanning, D. D., Beyer, C. E. and Painter, C. L., *FRAPCON-3: Modifications to fuel rod material properties and performance models for high-burnup application*, NUREG/CR-6534, PNNL-11513, Vol. 1, prepared for the U.S. Nuclear Regulatory Commission by Pacific Northwest Laboratory, Richland, Washington, 1997b.

Lassman K. and Benk, H., *Numerical algorithms for intragranular fission gas release,* J. Nuclear Materials, Vol 280, pp 127-135, 2000.

Lassman, K., O'Carrol, C., VanderLaar, J. and Walker, C.T., *The radial distribution of plutonium in high burnup UO_2 fuels*, J. Nuclear Materials, Vol. 228, pp. 223-231, 1994.

Limbäck, M.,*Comparison of models for Zircaloy cladding corrosion in PWR's*,
Halden Reactor Project Report HWR-468, Halden, Norway, March 1996.

Limbäck, M., Andersson, T., *A model for analysis of the effect of final annealing on the in- and out-of-reactor creep behavior of Zircaloy cladding*,
In: Proceedings of the Eleventh International Symposium on Zirconium in the Nuclear Industry, ASTM-STP-1295, pp. 448-468, 1996.

Lucuta, P.G:, Matzke, H.S. and Hastings, I.J., *A pragmatic approach to modeling thermal conductivity of irradiated UO_2 fuel: review and recommendations*,
J. Nuclear Materials, Volume 232, pp. 166-180, 1996.

Massih, A.R., Persson, S. and Weiss, Z., *Modelling of $(U,Gd)O_2$ fuel behaviour in boiling water reactors*, J. Nuclear Materials, Vol. 188, pp 323-330.

Mendelson, A., *Plasticity: theory and application*,
Krieger, New York, 1968.

Reif, F., *Fundamentals of statistical and thermal physics,*
McGraw-Hill, New York, 1965.

Ross-Ross, P.A. and Hunt, C.E.L., *The in-reactor creep of cold-worked Zircaloy-2 and Zirconium-2.5 wt% niobium pressure tubes,*
J. Nuclear Materials, Vol. 26, pp. 2-17, 1968.

Shann, S.H., Merckx, K.R., Lindenmeier, C.W., Lee, C.C. and Robinson A.H., *A two-group radial power distribution prediction model*, ANS-ENS International Topical Meeting on LWR Fuel Performance, Avignon, France, April 21-24, 1991, pp 578-587.

Todreas, N. and Jacobs, G., *Thermal contact conductance of reactor fuel elements*,
Nuclear Science and Engineering, Vol. 50, p. 283-, 1973.

Turnbull, J.A., *Review of nuclear fuel experimental data: fuel behaviour data available from IFE-OECD Halden project for development and validation of computer codes*,
OECD Nuclear Energy Agency report, ISBN 92-64-14422-6, 1995.

Turner, P.J., *ACE/gr user's manual,* SDS3, 91-3, Beaverton, Oregon, 1991.

Vitanza, C., *Comparison of correlations for fuel conductivity degradation*,
Halden Reactor Project F-Note 1049, Halden, Norway, 1995.

Appendix A: FRAPCON-3 fuel thermal conductivity model

The fuel thermal conductivity, λ_{fuel}, is correlated to the local temperature, burnup, Gd/Pu content and porosity through a model proposed by Lucuta *et al.* (1996)

$$\lambda_{fuel} = \lambda_0 F_D F_P F_M F_R . \tag{A1}$$

Here, λ_0 is the conductivity of unirradiated, fully dense fuel, F_D and F_P are burnup dependent corrections for dissolved and precipitated fission products in the fuel matrix, F_M is a correction factor for fuel porosity, and F_R is a temperature dependent compensation factor for irradiation effects. The conductivity of unirradiated fully dense fuel is calculated from a model given by Harding and Martin (1989)

$$\lambda_0 = \frac{10000}{375 + 2.165T} + \frac{4.715 \times 10^9}{T^2} e^{-16361/T}, \tag{A2}$$

where T is the temperature in Kelvin and λ_0 is in units of W/mK. The effects of dissolved and precipitated fission products on the conductivity are modeled by the factors

$$F_D = \left(\frac{1.09}{B^{3.265}} + \frac{0.0643\sqrt{T}}{\sqrt{B}} \right) \arctan\left(\left(\frac{1.09}{B^{3.265}} + \frac{0.0643\sqrt{T}}{\sqrt{B}} \right)^{-1} \right) \tag{A3}$$

and

$$F_P = 1 + \left(\frac{0.019B}{3 - 0.019B} \right) \left(1 + e^{\frac{1200-T}{100}} \right)^{-1}, \tag{A4}$$

where B is the fuel local burnup in atom% (1 atom% corresponds to 9.383 MWd/kgU at 200 MeV/fission). The effect of fuel porosity is accounted for by the Maxwell factor

$$F_M = \frac{1 - p}{1 + 0.5p}, \tag{A5}$$

where p is the volume fraction of porosity, stemming from fabrication and gaseous swelling. Irradiation decreases the fuel thermal conductivity at temperatures below 900-1000 K, and this irradiation effect is taken into account by the factor F_R

$$F_R = 1 - 0.2 \left(1 + e^{\frac{T-900}{80}} \right)^{-1}. \tag{A6}$$

It should be noticed, that this factor is applied at all times in the FRAPCON-3 model, also at the very first hours of fuel operation. In figures A1 and A2, λ_0 and F_R are shown with respect to temperature. The factors F_D and F_P are shown in figures A3 and A4.

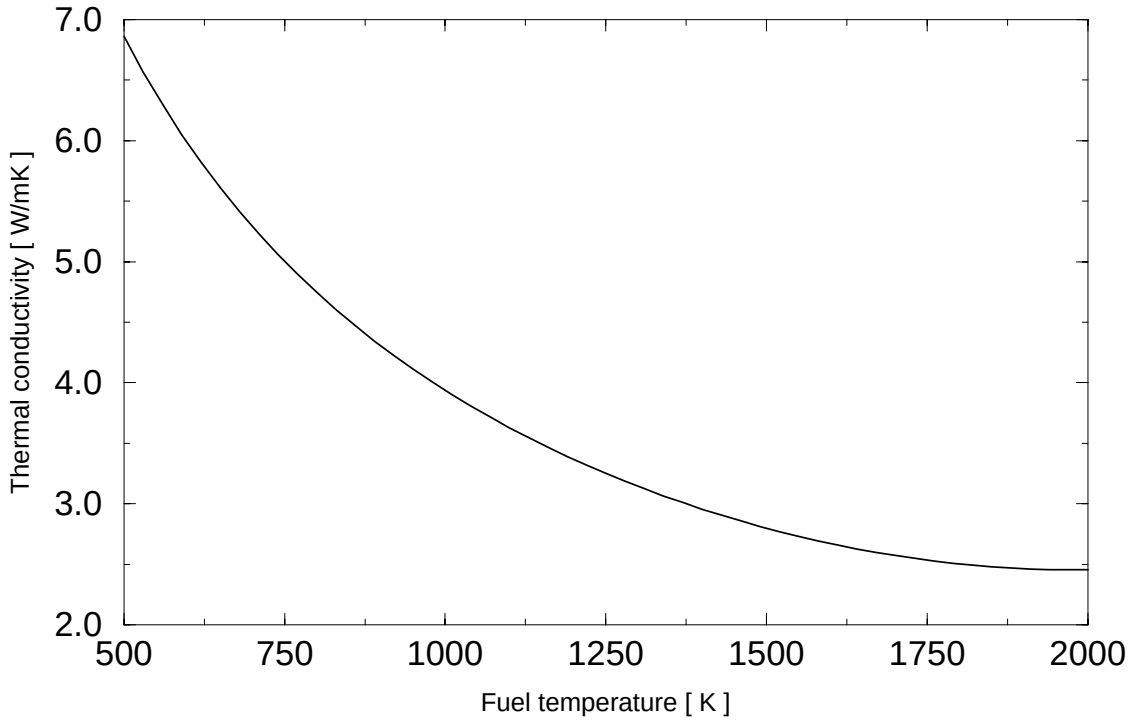

Figure A1: Thermal conductivity of unirradiated, fully dense UO_2 fuel, according to eq. (A2).

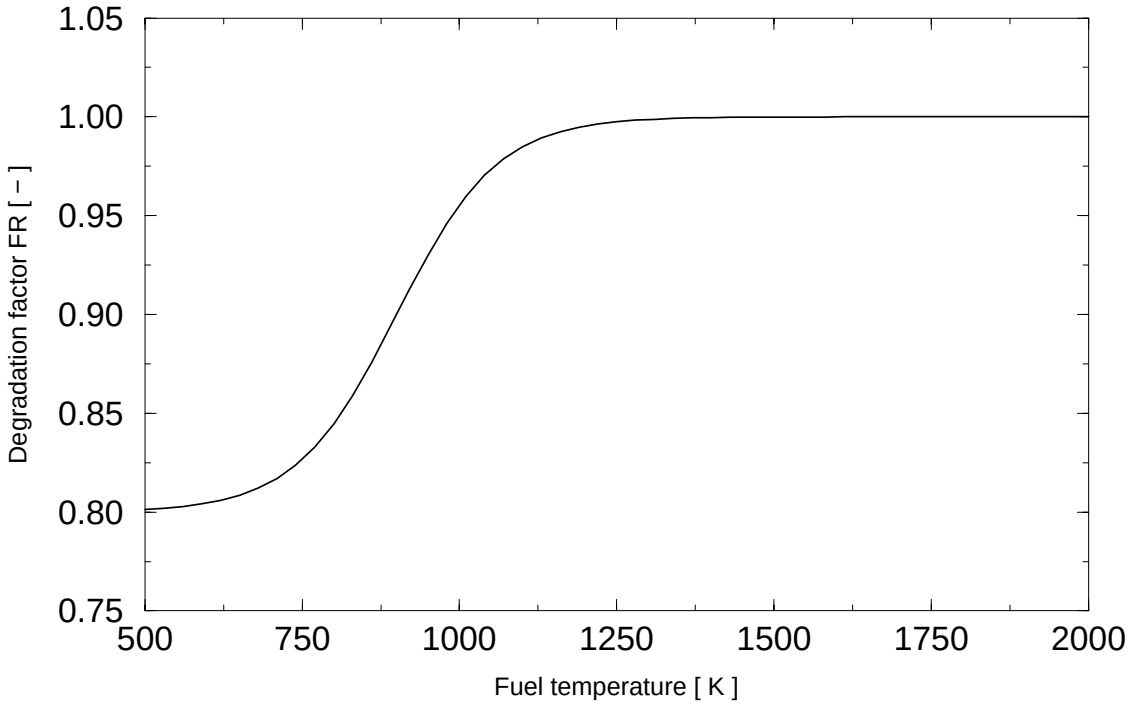

Figure A2: Irradiation-induced degradation factor F_R, according to eq. (A6).

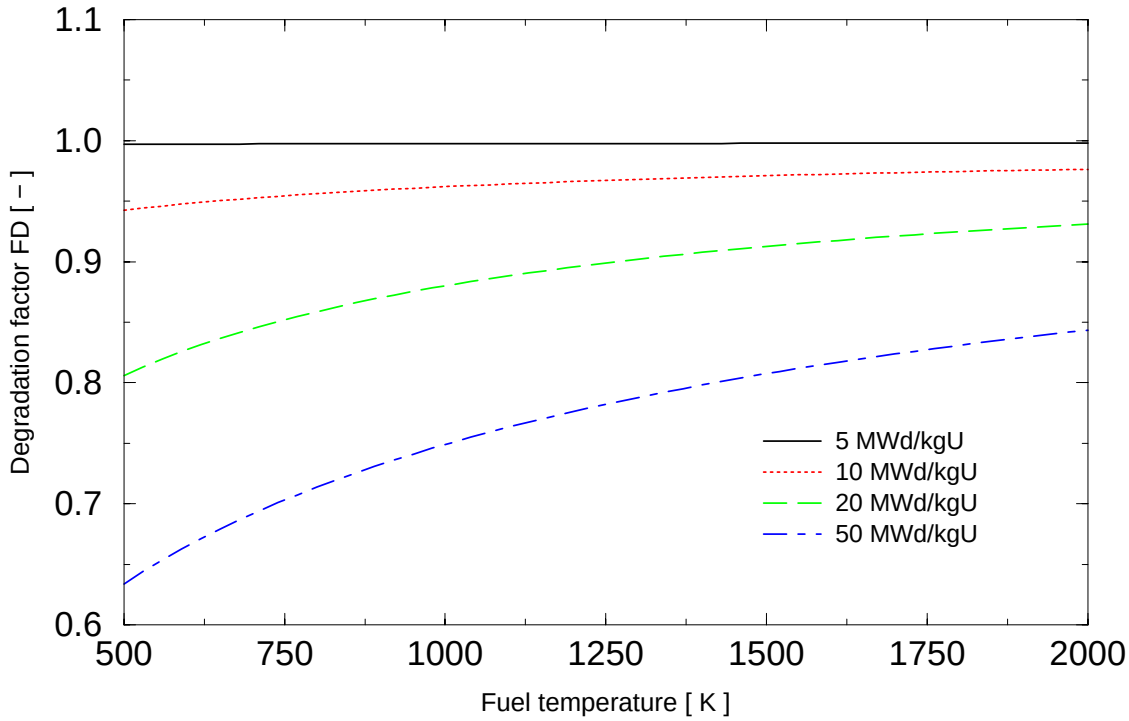

Figure A3: Degradation factor F_D, according to eq. (A3).

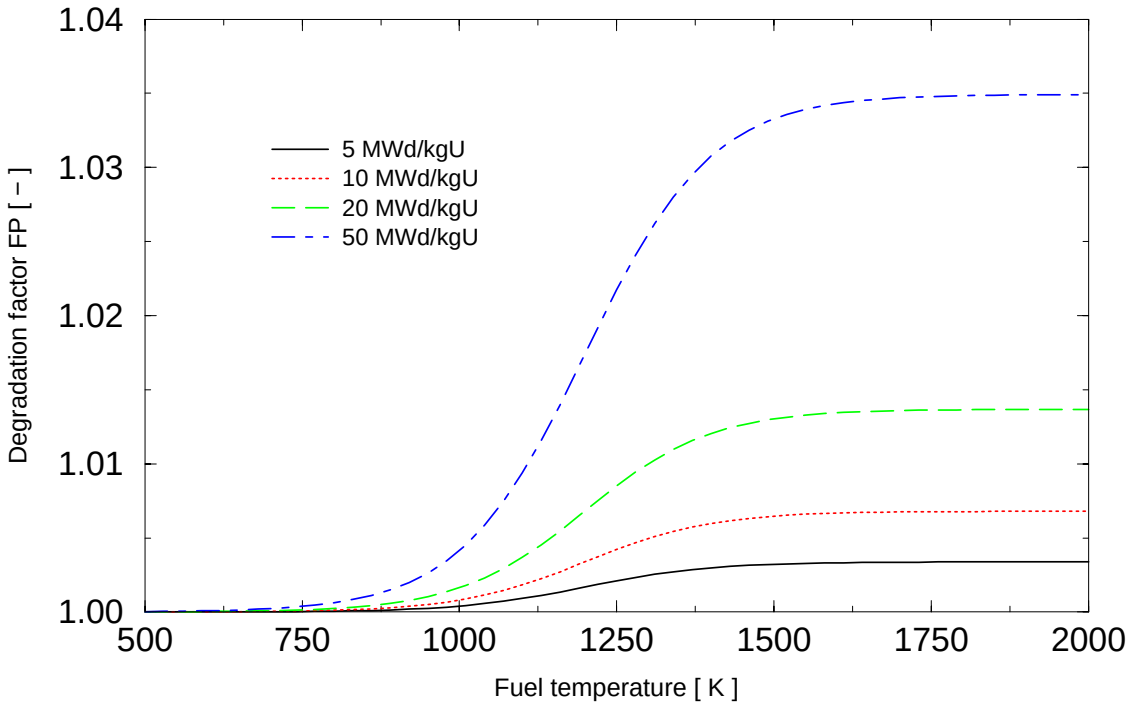

Figure A4: Degradation factor F_P, according to eq. (A4).

Appendix B: Halden fuel thermal conductivity model

In the Halden fuel thermal conductivity model, λ_{fuel} is correlated to the local temperature and burnup, Vitanza (1995). The correlation is

$$\lambda_{fuel} = \frac{4040}{190.85 + T + F_B} + 7.90 \cdot 10^{-3} e^{1.88 \cdot 10^{-3} T} . \qquad \text{(B1)}$$

Here, T is the fuel temperature in Kelvin and F_B is a burnup dependent correction factor

$$F_B = 10.67\, B_U - 4.66 \cdot 10^{-2} B_U^2 , \qquad \text{(B2)}$$

where B_U is the fuel local burnup in MWd/kgU. The fuel thermal conductivity predicted by this model is shown in figure B1 as a function of temperature and burnup.

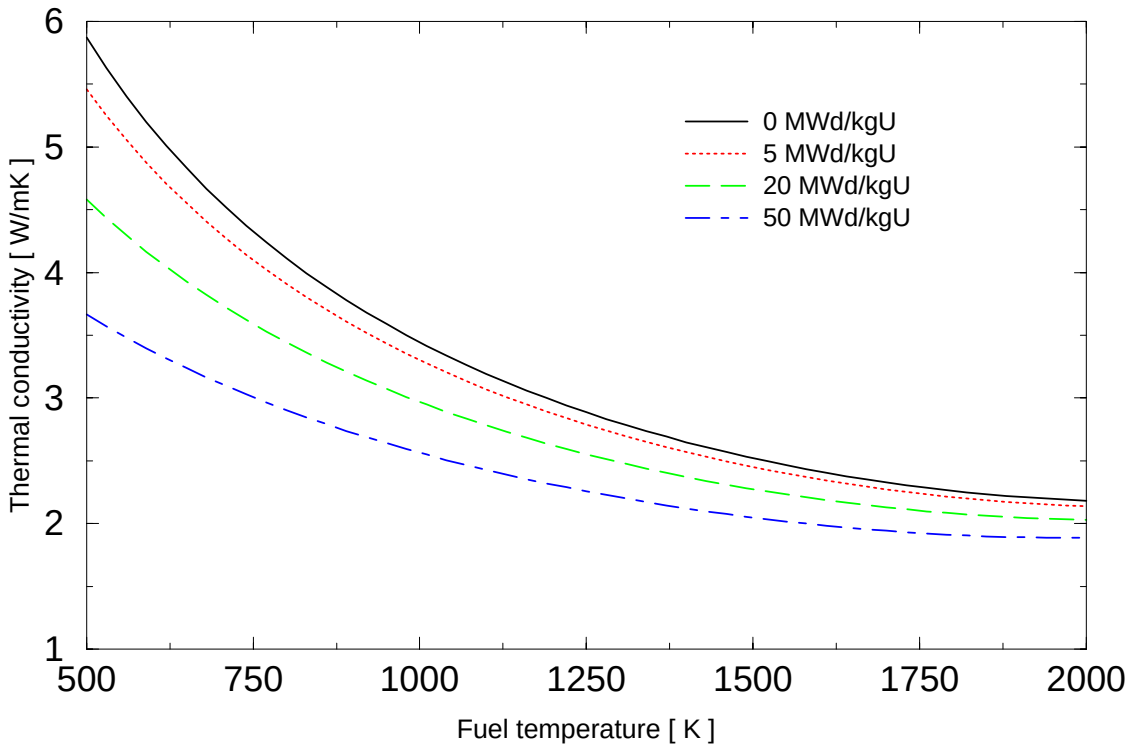

Figure B1: Fuel thermal conductivity according to eq. (B1).